

ตัวเร่งปฏิกิริยาอนุภาคนาโนโลหะฟอสไฟด์บนวัสดุรองรับแร่ดินเหนียวสำหรับ
การเปลี่ยนน้ำตาลเป็นสารอินทรีย์ที่มีมูลค่าเพิ่ม

Clay supported earth-abundant metal phosphide nanoparticles
catalyzing sugar conversion to value-added chemicals

โดย

นางสาวปัทมา ปรีตานรุฒิ

รายงานนี้เป็นส่วนหนึ่งของการศึกษาตามหลักสูตร

ปริญญาวิทยาศาสตรบัณฑิต

ภาควิชาเคมี คณะวิทยาศาสตร์

จุฬาลงกรณ์มหาวิทยาลัย

ปีการศึกษา 2563

Clay supported earth-abundant metal phosphide nanoparticles
catalyzing sugar conversion to value-added chemicals

Miss Patitta Preedanorawut

In Partial Fulfillment for the Degree of Bachelor of Science
Department of Chemistry, Faculty of Science
Chulalongkorn University
Academic Year 2020

Project Title: Clay supported earth-abundant metal phosphide nanoparticles catalyzing sugar conversion to value-added chemicals


Student name: Miss Patitta Preedanorawut

Accepted by Department of Chemistry, Faculty of Science, Chulalongkorn University in Partial Fulfillment of the Requirement for the Bachelor of Science.

PROJECT COMMITTEE

- | | |
|--|--------------------|
| 1. Assistant Professor Dr. Nipaka Sukpirom | Chair Committee |
| 2. Assistant Professor Dr. Rojrit Rojanathanes | Committee |
| 3. Dr. Junjuda Unruangsri | Project Advisor |
| 4. Assistant Professor Dr. Wipark Anutrasakda | Project Co-Advisor |

This report has been approved by the Head of the Department of Chemistry.



(Junjuda Unruangsri, D.Phil.)

Project Advisor



(Associate Professor Voravee P. Hoven, Ph.D.)

Head of Department of Chemistry



(Assistant Professor Wipark Anutrasakda, Ph.D.)

Project Co-Advisor

25 May 2021

ชื่อโครงการ ตัวเร่งปฏิกิริยาอนุภาคนาโนโลหะฟอสไฟด์บนวัสดุรองรับแร่ดินเหนียวสำหรับการ
เปลี่ยนน้ำตาลเป็นสารอินทรีย์ที่มีมูลค่าเพิ่ม

ชื่อนิสิตในโครงการ นางสาวปติตตา ปรีดานรุธิ เลขประจำตัว 6033057023

ชื่ออาจารย์ที่ปรึกษา อาจารย์ ดร. จัญจุตา อุ่นเรืองศรี

ชื่ออาจารย์ที่ปรึกษาร่วม ผู้ช่วยศาสตราจารย์ ดร. วิภาค อนุตรศักดิ์ดา

ภาควิชาเคมี คณะวิทยาศาสตร์ จุฬาลงกรณ์มหาวิทยาลัย ปีการศึกษา 2563

บทคัดย่อ

การเปลี่ยนน้ำตาลสามารถผลิต 5-ไฮดรอกซีเมทิลเฟอร์พิวรัล และอนุพันธ์ได้ ซึ่งสารดังกล่าวสามารถนำมาใช้เพื่อเปลี่ยนเป็นสารเคมีที่มีมูลค่าเพิ่มขึ้น ในปัจจุบัน มีรายงานเกี่ยวกับการนำตัวเร่งปฏิกิริยาเอกพันธ์และตัวเร่งปฏิกิริยาวิวิธพันธ์มาใช้ในการเร่งปฏิกิริยาการเปลี่ยนน้ำตาลให้มีประสิทธิภาพในการเร่งปฏิกิริยาและมีความจำเพาะต่อปฏิกิริยาดังกล่าว ในงานวิจัยนี้จึงมีจุดประสงค์ในการเปลี่ยนน้ำตาลกลูโคสและฟรุกโตสให้เป็น 5-ไฮดรอกซีเมทิลเฟอร์พิวรัล และผลิตภัณฑ์ที่มีมูลค่าเพิ่มขึ้นตามลำดับ ดังนั้นจึงได้มีการนำแร่ดินเหนียวมอนต์โมริลโลไนต์ที่ถูกแลกเปลี่ยนโดยไอออนของโครเมียม (III) มารวมกับอนุภาคนาโนโลหะฟอสไฟด์เพื่อให้เป็นตัวเร่งปฏิกิริยาเพียงตัวเดียว โดยเริ่มจากการสังเคราะห์อนุภาคนาโนโลหะฟอสไฟด์โดยให้ความร้อนเกลือคลอไรด์ของโลหะนิกเกิล และ/หรือ โครเมียมและสารลดแรงตึงผิวต่าง ๆ จากนั้นนำไปกระจายตัวบนแร่ดินเหนียวมอนต์โมริลโลไนต์ที่ถูกแลกเปลี่ยนโดยไอออนของโครเมียม (III) ตัวเร่งปฏิกิริยาที่สังเคราะห์ได้ถูกนำมาพิสูจน์เอกลักษณ์ด้วยเทคนิคทางสเปกโทรสโกปีต่าง ๆ เพื่อยืนยันโครงสร้างทางเคมี ความสามารถในการเร่งปฏิกิริยานั้น ได้ศึกษาผลของตัวทำละลายของเหลวไอออนิกต่างชนิดกัน ได้แก่ N-เมทิลอิมิดาโซเลียมคลอไรด์ ([HMIM]Cl), 1-บิวทิล-3-เมทิลอิมิดาโซเลียมคลอไรด์ ([BMIM]Cl) และ N-เมทิลอิมิดาโซเลียมไฮโปซัลเฟต ([HMIM][HSO₄]) ผลการทดลองพบว่าตัวทำละลายของเหลวไอออนิกชนิด [HMIM]Cl ให้สารผลิตภัณฑ์มากที่สุดเมื่อเปรียบเทียบกับตัวทำละลายของเหลวไอออนิกชนิดอื่น นอกจากนี้ทุกตัวเร่งปฏิกิริยา (ตัวเร่งปฏิกิริยาแร่ดินเหนียว Cr-K10, ตัวเร่งปฏิกิริยา Ni₂P/Cr-K10 และ ตัวเร่งปฏิกิริยา Ni₂P ที่ผสมกับแร่ดินเหนียว Cr-K10) ให้ร้อยละผลผลิต 5-ไฮดรอกซีเมทิลเฟอร์พิวรัล จากน้ำตาลฟรุกโตสมากกว่า 60 ภายใน 1.5 ชั่วโมง ส่วนผลผลิตที่ได้จากน้ำตาลกลูโคสยังไม่เป็นที่น่าพอใจ ดังนั้น จึงสามารถระบุได้ว่า Ni₂P/Cr-K10 เป็นตัวเร่งปฏิกิริยาที่ดีและสามารถนำไปใช้ในปฏิกิริยาการเปลี่ยนเป็นสารอื่นที่มีมูลค่าเพิ่มได้ในภายหน้า

คำสำคัญ: ตัวเร่งปฏิกิริยาวิวิธพันธ์; กลุ่มแร่ดินเหนียวมอนต์โมริลโลไนต์; กลูโคส; ฟรุกโตส;
ตัวทำละลายของเหลวไอออนิก; การแปลงสภาพน้ำตาล; อนุภาคนาโนโลหะฟอสไฟด์;
5-ไฮดรอกซีเมทิลเฟอร์พิวรัล

Project Title Clay supported earth-abundant metal phosphide nanoparticles catalyzing sugar conversion to value-added chemicals

Student Name Miss Patitta Preedanorawut Student ID 6033057023

Advisor Name Junjuda Unruangsri, D.Phil.

Co-advisor Name Assistant Professor Wipark Anutrasakda, Ph.D.

Department of Chemistry, Faculty of Science, Chulalongkorn University, Academic Year 2020

Abstract

Sugar conversion can produce high value-added chemicals such as HMF, levulinic acid, formic acid and other derivatives. Successful sugar conversion was witnessed using both heterogeneous and homogeneous catalysts, giving mostly one-step converted products. This work aims to transform monosaccharides (i.e., glucose and fructose) to HMF and HMF-reduced products such as BHMF through a one-pot tandem catalysis. Therefore, an acid-catalyzed Cr-exchanged montmorillonite K10 clay (Cr-K10) and a hydrogenate metal phosphide nanoparticles ($\text{Ni}_x\text{Co}_{2-x}\text{P}$) were combined. Metal phosphide nanoparticles were thermally synthesized using Ni(II) and/or Co(II) salt with phosphite salt, in the presence of surfactants. The NPs were later dispersed on to the surface of Cr-K10. The synthesized catalysts were characterized by several spectroscopic techniques to confirm the chemical structure. In addition, effects of different types of ionic liquids including N-methylimidazolium chloride ([HMIM]Cl), 1-butyl-3-methylimidazolium chloride ([BMIM]Cl) and N-methylimidazolium bisulfate ([HMIM][HSO₄]) on the catalytic activity were investigated. Due to the time limit, the catalytic performance towards conversion of sugar into HMF was only examined. Results demonstrated that using [HMIM]Cl as medium provided the highest yield of HMF compared to other ionic liquids. Furthermore, over 60% yields of HMF from fructose were obtained in all catalysts (Cr-K10, Ni₂P/Cr-K10 and Ni₂P mixed with Cr-K10) at 120 °C within 1.5 h, while the HMF yields from glucose were unsatisfyingly achieved. This suggested that the synthesized Ni₂P/Cr-K10 is found to be a good catalyst and can be potentially applicable for further conversion to other value-added chemicals in the next step.

Keywords: Heterogeneous catalyst; Montmorillonite; Glucose; Fructose; Ionic liquid; Sugar conversion; Metal phosphide nanoparticles; 5-Hydroxymethylfurfural

ACKNOWLEDGEMENTS

I would like to express my deep and sincere gratitude towards my project advisor and co-advisor, Dr. Junjuda Unruangsri and Assistant Professor Dr. Wipark Anutrasakda, respectively, for giving me the opportunity to conduct this research and providing invaluable guidance throughout the course of study. This project would not be accomplished without their exceptional support, encouragement, and instruction with kindness. Besides my project advisor and co-advisor, I would also like to thank my project committees: Assistant Professor Dr. Nipaka Sukpirom and Assistant Professor Dr. Rojrit Rojanathanes, for their insightful comments and hard questions.

My sincere thank also goes to my seniors in JU lab, especially Dr. Ratanakorn Teerasarunyanon, for their endless support, kindness and encouragement. Thanks to all their good advice and support that helped me complete this work perfectly.

I would like to thank my fellow classmates in Department of Chemistry, Faculty of Science, Chulalongkorn University who gave the good advice and also encouraged me to get through the tough times during working this study.

Last but not least, I would like to extend my appreciation to my family: my parents and sisters, who are always by my side anytime I needed. I am extremely grateful to them for their love, caring, understanding and continuing support.

Miss Patitta Preedanorawut

CONTENTS

ABSTRACT IN THAI	IV
ABSTRACT IN ENGLISH	V
ACKNOWLEDGEMENTS	VI
LIST OF FIGURES.....	IX
LIST OF SCHEMES.....	X
LIST OF TABLES	XI
CHAPTER I INTRODUCTION AND LITERATURE REVIEWS	1
1.1. Introduction.....	1
1.2. Objectives and Scopes of this research.....	3
1.2.1. Objectives of this research.....	3
1.2.2. Scopes of this research.....	3
1.3. Theory and Literature Reviews	4
1.3.1. Biomass conversion route	4
1.3.2. Montmorillonite K10 clay	5
1.3.3. Metal phosphides.....	6
1.3.4. Ionic liquids.....	8
CHAPTER II EXPERIMENTS.....	9
2.1. General experimental details.....	9
2.2. Catalyst preparation	9
2.2.1. Synthesis of $\text{Ni}_x\text{Co}_{2-x}\text{P}$ NPs.....	9
2.2.2. Preparation of Cr-K10	10
2.2.3. Preparation of $\text{Ni}_x\text{Co}_{2-x}\text{P}/\text{Cr-K10}$	10
2.3. Synthesis of ionic liquid	10
2.3.1. Synthesis of [HMIM]Cl.....	11
2.3.2. Synthesis of [BMIM]Cl	11
2.3.3. Synthesis of [HMIM][HSO_4].....	12
2.4. Catalytic reaction procedure.....	12

CHAPTER III RESULTS AND DISCUSSION.....	13
3.1. Characterizations of catalyst.....	13
3.1.1. Characterizations of Ni _x Co _{2-x} P NPs.....	13
3.1.2. Characterization of Cr-K10.....	15
3.1.3. Characterization of Ni _x Co _{2-x} P/Cr-K10.....	17
3.1.4. N ₂ adsorption–desorption study.....	18
3.1.5. Elemental composition study.....	19
3.2. Characterization of ionic liquids.....	20
3.3. The catalytic studies towards sugar conversion to HMF.....	23
3.3.1. Determination of optimal ionic liquid media for glucose conversion.....	23
3.3.2. Conversion of glucose and fructose to HMF using Cr-K10 as catalyst.....	24
3.3.3. Conversion of glucose and fructose to HMF using Ni ₂ P/Cr-K10 as catalyst.....	26
3.3.4. Conversion of glucose and fructose to HMF using Ni ₂ P mixed with Cr-K10.....	27
CHAPTER IV CONCLUSIONS.....	28
REFERENCES.....	29
APPENDIX.....	33
VITA.....	39

LIST OF FIGURES

Figure 1-1: Basic framework of the biorefinery process based on HMF.....	5
Figure 1-2: Interlayer distance and basal spacing in montmorillonite:.....	6
Figure 2-1: Chemical structures of the used ionic liquids.....	11
Figure 2-2: Synthesis procedure for [HMIM]Cl.	11
Figure 2-3: Synthesis procedure for [BMIM]Cl.....	11
Figure 2-4: Synthesis procedure for [HMIM][HSO ₄].	12
Figure 3-1: XRD pattern of the synthesized (a) Ni ₂ P (b) Co ₂ P (c) NiCoP NPs.....	14
Figure 3-2: TEM images of (a) Ni ₂ P (b) Co ₂ P (c) NiCoP NPs.....	15
Figure 3-3: XRD pattern of K10-MMT and the prepared Cr-K10.....	16
Figure 3-4: FT-IR spectra of K10-MMT and the prepared Cr-K10.....	17
Figure 3-5: TEM images of Ni ₂ P/Cr-K10.....	18
Figure 3-6: The N ₂ adsorption–desorption isotherms spectra of K10-MMT, the prepared Cr-K10 and the synthesized Ni ₂ P/Cr-K10.....	19
Figure 3-7: ¹ H NMR spectra of the synthesized [HMIM]Cl, [BMIM]Cl and [HMIM][HSO ₄].....	21
Figure 3-8: FT-IR spectra of the synthesized [HMIM]Cl, [BMIM]Cl and [HMIM][HSO ₄].	22
Figure 3-9: Stacked ¹ H NMR spectra of glucose conversion for 1 h using Cr-K10 catalyst in [HMIM][HSO ₄], [HMIM]Cl and [BMIM]Cl as media.....	24

LIST OF SCHEMES

Scheme 1-1: The one-pot tandem reaction of sugar hydrolysis route.	3
Scheme 1-2: Plausible Reaction Pathway for the Conversion of 5-methylfurfural into 2,5-hexanedione over Ni ₂ P NPs.....	7
Scheme 3-1: Glucose and fructose conversion to HMF.....	23

LIST OF TABLES

Table 3-1: Surface properties of K10-MMT, the prepared Cr-K10 and the synthesized Ni ₂ P/Cr-K10.....	19
Table 3-2: The elemental analysis of the synthesized Cr-K10, Ni ₂ P NPs and Ni ₂ P/Cr-K10 determined by ICP-OES.....	20
Table 3-3: Yield of HMF from glucose and fructose conversion using Cr-K10 catalyst in [HMIM]Cl medium at different reaction time.....	25
Table 3-4: Yield of HMF from glucose and fructose conversion using Ni ₂ P/Cr-K10 catalyst in [HMIM]Cl medium at different reaction time.....	26
Table 3-5: Yield of HMF from glucose and fructose conversion using Ni ₂ P mixed with Cr-K10 catalyst in [HMIM]Cl medium at different reaction time.	27

Chapter I

Introduction and literature reviews

1.1. Introduction

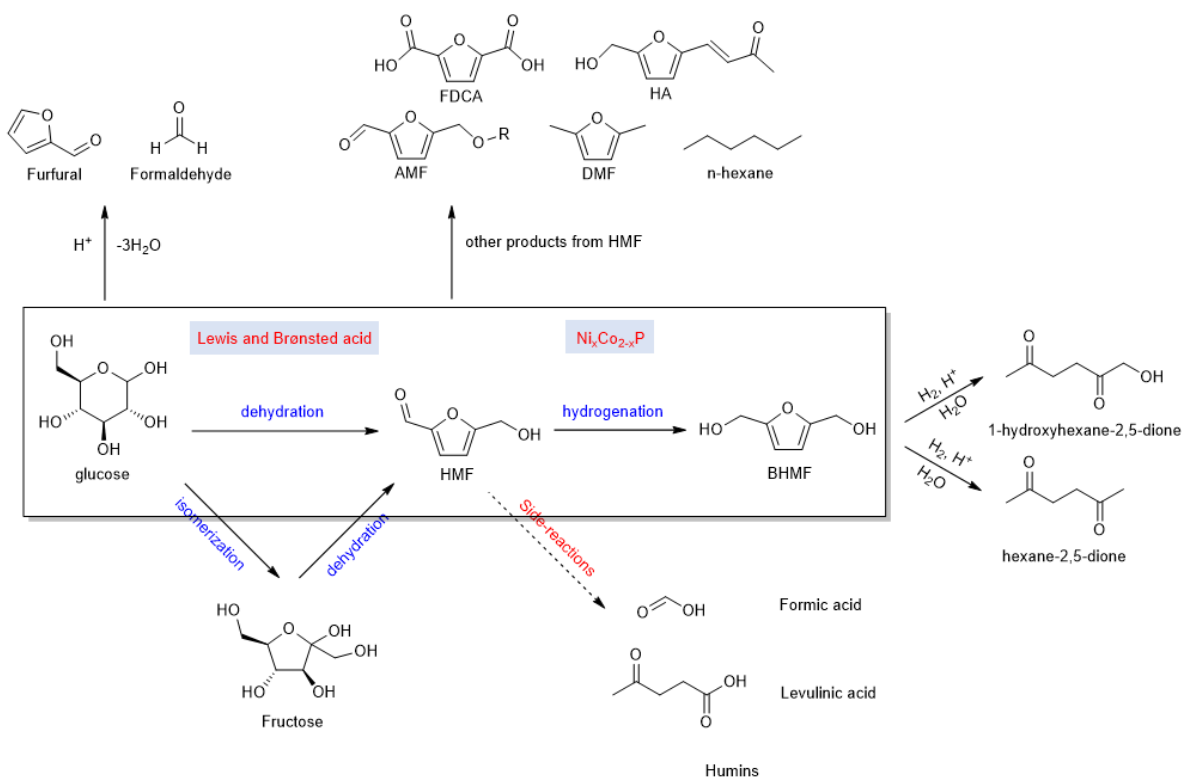
Biomass is a plentiful and carbon-neutral renewable energy resource. It is being intensely investigated as feedstock for the production of biofuels and valuable chemicals of the future, which will replace fossil-based resources. The direct use of real biomass can lead to less energy consumption and less CO₂ emissions. Most of carbohydrates represent the renewable biomass. The most widespread monosaccharide is glucose which is produced by photosynthesis and is the most abundant component in the plants, resulting in its low commercial price. The utilization of glucose to generate valuable compounds effectively, such as furfural and formaldehyde¹, is a very important topic. 5-Hydroxymethylfurfural (HMF) is found to be an intermediary connecting biomass raw materials to the biorefinery industry. Hence, HMF is an important biomass-based compound which can be further used to synthesize high value-added chemicals² such as 2,5-diketone, which plays an important role in biorefining technology and is valuable intermediates for many chemical compounds³ (**Scheme 1-1**).

HMF is the primary product obtained from the acid-catalyzed dehydration of C₆-sugar molecules.⁴ It was proved that the conversion of fructose to HMF is more facile than that of glucose. Though a low yield of HMF is obtained, glucose, which is derived from carbohydrates, is the preferred raw material used for producing HMF, due to its higher availability and lower prices.^{5,6} Hence, an effective catalytic system has been considerable as an approach for producing HMF from glucose in high yields. Precedent literature demonstrates that various forms of Lewis and Brønsted acids are often employed in the conversion of sugar to HMF. At present, some homogeneous catalysts are reported to obtain higher HMF yield such as ionic liquid, mineral acid, inorganic and organic acid, and metal salts (CrCl₂, CrCl₃).⁷ Meanwhile heterogeneous catalysts have been developed for converting glucose to HMF due to their advantageous reusability without a significant loss in activity and selectivity such as metal oxides, phosphates, zeolite and polymer-based catalysts.⁸ Cation-exchanged montmorillonite K10 clay (K10-MMT) has also been reported as supporting material for many applications due to its low cost and significant cation-exchange ability of its structure.⁹ Consequently, chromium-exchanged montmorillonite K10 clay (Cr-K10) is the good candidate of

heterogeneous catalyst used to catalyze the conversion of glucose into HMF.¹⁰ To afford excellent HMF yield, Brønsted acid ionic liquids, N-methylimidazolium chloride ([HMIM]Cl), 1-butyl-3-methylimidazolium chloride ([BMIM]Cl) and N-methylimidazolium bisulfate ([HMIM][HSO₄]), have been discovered as reaction media in order to prohibit decomposition of HMF, help stabilize HMF products and promote the selective dehydration of sugar into HMF.^{11,12}

Some of other upgrading of HMF towards value-added fuels and chemical commodities, including furan derivatives, fuel additives, dicarboxylic acids and hydrocarbons are presented in the **Scheme 1-1**, which are produced by using different catalysts in each product via selective oxidation, hydrogenation, etherification, coupling and condensation reaction¹. Recently, metal phosphide nanoalloys, such as nickel (Ni₂P) and cobalt phosphides (Co₂P), have attracted much attention as highly effective catalysts for the selective transformation of biofuranic aldehydes to diketones through the hydrogenation reaction.¹³ As described above, the designable one-pot tandem catalyst used for sugar hydrolysis to produce HMF and subsequent diketone derivatives of HMF is considerably challenging. Hence, the combination of two catalysts, Cr-K10 and metal phosphide nanoalloys which provide both properties; acid and hydrogenation catalysts, would be a good match in the route synthesis from glucose to diketone derivatives as shown in the **Scheme 1-1**.

However, tandem catalysts reviewed in harsh and long time-consuming reaction, high temperature and/or pressure, such as 100 °C under 50 bar in 32 h,¹⁴ is still a research gap. To fill this gap, the more effective catalyst with milder conditions required in this conversion reaction would be beneficial. Hence, Cr-K10 is combined with Ni_xCo_{2-x}P by two step procedure, synthesis of Ni_xCo_{2-x}P from heated Ni and/or Co salts and surfactants firstly and then followed by dispersing them into Cr-K10. Then, catalytic activity toward sugar conversion to subsequent derivatives of HMF, which is investigated in mentioned ionic liquid at 120 °C under atmospheric pressure within only 3 h, is the scope of this work.



Scheme 1-1: The one-pot tandem reaction of sugar hydrolysis route.

1.2. Objectives and Scopes of this research

1.2.1. Objectives of this research

To develop efficient catalysts based on $\text{Ni}_x\text{Co}_{2-x}\text{P}$ nanoparticles supported Cr-exchanged montmorillonite K10 clay for conversion of sugar to value-added chemicals.

1.2.2. Scopes of this research

- Preparation of $\text{Ni}_x\text{Co}_{2-x}\text{P}$ NPs (when $x = 1$ and 2).
- Preparation of Cr-exchanged montmorillonite K10 clay (Cr-K10).
- Synthesis of $\text{Ni}_x\text{Co}_{2-x}\text{P}/\text{Cr-K10}$ and characterization using XRD, TEM, FT-IR, ICP-OES, and BET surface area analyzer.
- Synthesis of ionic liquids, including [HMIM]Cl, [BMIM]Cl and [HMIM][HSO₄] and characterization using FT-IR and ¹H NMR.
- The study of catalytic performances towards conversion of glucose and fructose into HMF using Cr-K10, $\text{Ni}_2\text{P}/\text{Cr-K10}$ and Ni_2P mixed with Cr-K10 ($\text{Ni}_2\text{P} + \text{Cr-K10}$) in the variety of ionic liquids, including [HMIM]Cl, [BMIM]Cl and [HMIM][HSO₄] as media.
- Characterization and yield calculation of produced HMF by ¹H NMR.

1.3. Theory and Literature Reviews

1.3.1. Biomass conversion route

Biomass is renewable organic material that comes from plants and animals which contains stored chemical energy from the sun through photosynthesis such as carbohydrates, lignin, fatty acids, lipids, proteins, and so on. Lignocellulosic biomass, found in the cell walls of plants, is the most abundant and available biomass source for biorefineries.¹⁵ From previous reports, it has been investigated that lignocellulosic biomass was used to transform into useful products in biorefinery technologies, which has potential to replace petroleum refining. Biomass can be burned directly for heat or converted to renewable liquid and gaseous fuels through various processes. The conversion of biomass to final products requires a series of deconstruction, catalytic conversion, separation and purification processes. From the **Figure 1-1**, HMF is found to be an intermediary connecting biomass raw materials to the biorefinery industry, which can be converted into multiple target products.¹ Glucose can be obtained from cellulose via acid-catalyzed hydrolysis. After removing three molecules of water from glucose, HMF can be obtained, which can be further converted to versatile products covering an extensive range of structures and applications.^{16, 17} Therefore, the development of environmentally friendly and effective catalytic technology that can convert cellulose into HMF and its subsequent conversion to value-added chemicals has been popular issues among researchers for the last few decades. Also, many interesting results have been recently published on the development and applications of new materials and solvents for the synthesis and upgrading of HMF.

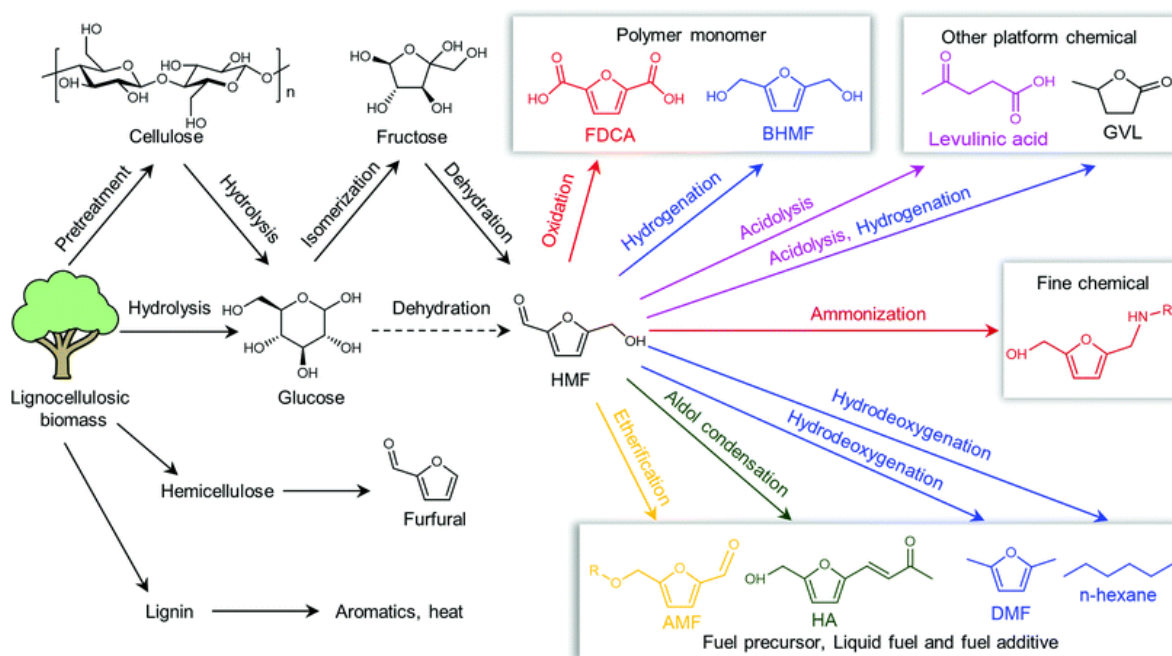


Figure 1-1: Basic framework of the biorefinery process based on HMF.¹

1.3.2. Montmorillonite K10 clay

Montmorillonite K10 clay (K10-MMT) is a silicate mineral that was contained in nature and it was an abundant amount. In general, clay minerals are basically consisted of multiple layers of hydroxylated and coordinated tetrahedral and octahedral sheets.¹⁸ In K10-MMT, it is composed of aluminosilicate layers, where one octahedral alumina sheet is sandwiched between two tetrahedral silica sheets. The distance between the two layers is known as interlayer distance or gallery height, while interlayer distance with thickness of a single aluminosilicate layer constitutes the basal spacing as shown in the **Figure 1-2**. These cations in the interlayer are highly exchangeable, thus K10-MMT is able to accommodate various guest molecules in its interlayer space. Due to these structural features, K10-MMT can efficiently behave as a support by introducing many guest species between the layers or on its external surface. Various cationic species can be introduced into its narrow interlayers by simple ion-exchange methods, so it is easy to modify into catalyst support material.^{19, 20}

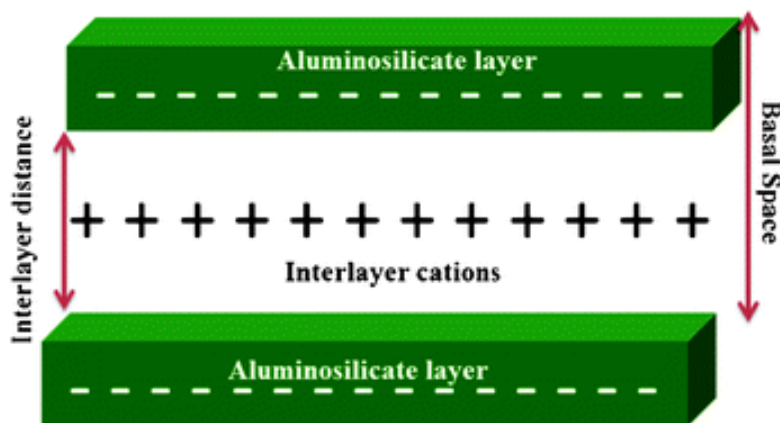


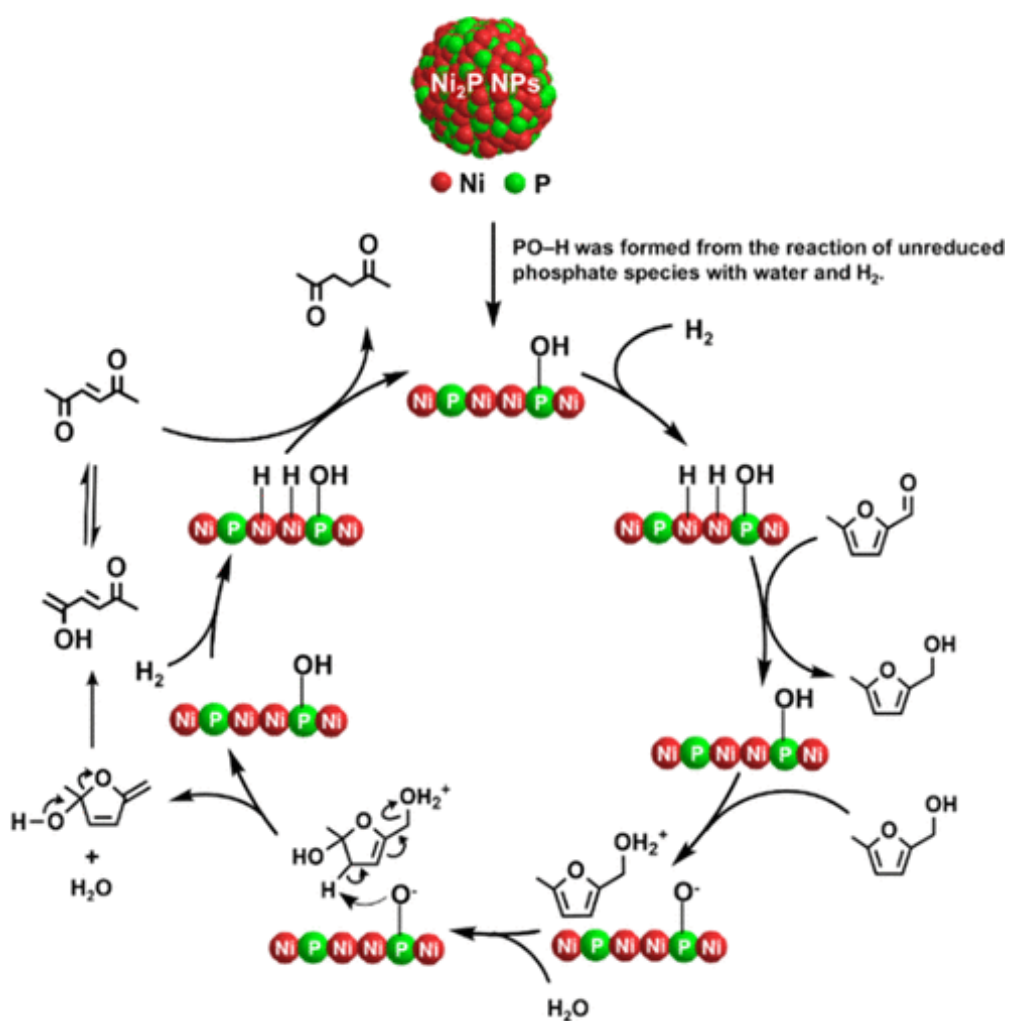
Figure 1-2: Interlayer distance and basal spacing in montmorillonite.¹⁰

During the last decade, the synthesis of nanomaterials has attracted a lot of attention in materials research. It is because they exhibit specific properties (optical, electronic, magnetic, and so on) than those of individual atoms or their bulk counterparts due to quantum size and surface effects, which makes them particularly attractive candidates for many applications. Immobilization of metal nanoparticles on appropriate supports has generated considerable attention due to the potential for control of nanoparticle size, shape and activity. Another advantage of nanoparticle immobilization on solid support is nanoparticle aggregation inhibition. In this regard, nanoparticle/clay composites are an active field of research¹⁰. In 2008, there are public reports about the use of K10-MMT supported metal nanoparticles for many applications. For instance, catalytic activity of 14 types of metal ion-exchanged K10-MMT was tested for the acetylation of cyclohexanol with acetic anhydride at room temperature by K. -i. Shimizu *et al.*²¹ In 2013, Zhongfeng Fang *et al.* developed the conversion of carbohydrate into HMF by using chromium-exchanged K10-MMT clay (Cr-K10) as catalyst.¹¹ This successful discovery was also confirmed in different reaction solvents with high HMF yield by Aziz Rahman Aylak *et al.* in 2019.²²

1.3.3. Metal phosphides

Transition metal phosphides (such as FeP, MoP, Co₂P, CoP, NbP and Ni₂P) have drawn attentions for many applications in energy storage,²³ optics,²⁴ magnetism²⁵ and catalysts.²⁶ The phosphorus atom in transition metal phosphides is usually found at the center of a triangular prism, rather than locating between metal host atoms due to its large atomic radius (0.109 nm). Moreover, phosphides have many coordination unsaturated bonds, resulting in their many phase states.²⁷ Transitional metal phosphides present better catalytic effects for

hydrodesulfurization (HDS), and hydrogen evolution reaction (HER) processes.²⁸ Recently, Nickel (Ni_2P) and cobalt (Co_2P) phosphides are most commonly used as catalysts for biomass conversion. In 2020, T. Mitsudome *et al.* demonstrated the high catalytic activity and selectivity of Ni_2P nanoparticles for the transformation of HMF derivatives to 2,5- diketones in water without any additives and proposed a possible reaction pathway for the transformation as shown in the **Scheme 1-2**. And in the next year, the same group has been reported good results of a supported nano- Co_2P as an efficient heterogeneous catalyst for the selective hydrogenation of furfural derivatives. Furthermore, transition bimetal phosphide-based catalysts have also been widely explored. Among ternary phosphides, $\text{Ni}_x\text{Co}_{2-x}\text{P}$ has been researched extensively and demonstrated as an highly efficient catalysts for the HER²⁹ but there are still no reports about the use of $\text{Ni}_x\text{Co}_{2-x}\text{P}$ for HMF transformation until now.



Scheme 1-2: Plausible Reaction Pathway for the Conversion of 5-methylfurfural into 2,5-hexanedione over Ni_2P NPs.³

1.3.4. Ionic liquids

Ionic liquids are organic salts in the liquid state, which usually consist of an organic cation and a polyatomic inorganic anion. Their physical and chemical properties can be modified by the selection of the cation and anion compositions. Ionic liquids have been recognized as environmentally friendly alternative to volatile organic solvents.³⁰ Applications of ionic liquids in chemical processes have been widely studied within the last decade. The potential for selectively making HMF from glucose using ionic liquids as reaction solvents was first demonstrated in 2007 by Zhao *et al.* This study indicated the ability of various metal salts to convert glucose into HMF in 1-ethyl-3-methylimidazolium chloride ([EMIM]Cl). They found that chromium salts (CrCl_2) were the most active catalysts, affording up to 70% HMF yield at 100°C within 3 h. This is better than most yields obtained in aqueous systems.³¹ Additional reports of glucose conversion to HMF using different catalysts in ionic liquids (mostly imidazolium chloride) were done by many researchers because of the high solubility of carbohydrates. For instance, a variety of zeolite catalysts were examined in 1-butyl-3-methylimidazolium chloride ([BMIM]Cl) and produced 50% HMF yield at 150°C in only 50 min, which is the highest catalytic activity. Ionic liquids have also been explored as additives/co-solvents rather than as the single liquid solvent for the reaction. In 2012, X. Qi *et al.* attempted to use 1:1 of $[\text{C}_6\text{C}_1\text{im}]\text{Cl}$ /water as biphasic mixtures in glucose conversion, and HMF yields of 53% were obtained within just 10 min at 200°C in the presence of ZrO_2 .³² It is clear that different ionic liquid systems can provide a solid effect on catalyst activity and byproduct formation.

Chapter II

Experiments

2.1. General experimental details

All chemicals and solvents used in this research were commercially available and used as received without further purification, unless noted otherwise. Powder X-ray diffraction (PXRD) patterns were measured at 2θ in a range of 20-80 degrees by a Rigaku, Smartlab 30kV diffractometer equipped with a fixed monochromator and a Cu-K α radiation source which was set an accelerating voltage of 40 kV, an applied current of 30 mA and a scan speed of 5 deg/min. Transmission Electron Micrographs were taken on the Transmission Electron Microscope (TEM, JEOL JEM-1400). All FT-IR spectra were recorded by Fourier Transform Infrared Spectrometer (FT-IR) by the Perkin Elmer at wavenumber range 4000-400 cm^{-1} using KBr pellet technique. Pore parameters of the synthesized catalysts were evaluated from nitrogen adsorption-desorption method (BELSORP, mini-II nitrogen absorptiometer). ^1H NMR spectra were recorded on the JEOL 500 MHz spectrometer at ambient temperature. ^1H NMR chemical shifts were given relative to tetramethyl silane (TMS) and referenced to the solvent signal. Mestre nova software (version 6.0.2-5475) was used to process and analyze the spectra.

Inductively coupled plasma optical emission spectrometric measurements were carried out on Thermo Scientific, model iCAP 6500 series ICP-OES Spectrometer. To prepare the sample for ICP-OES analysis, the exact amount of the sample was digested by adding with 3 mL of concentrated nitric acid in a large-mouth glass container under magnetic stirring at ambient temperature overnight. After that, the solution was heating to remove concentrated nitric acid. The sample was obtained and diluted with 1% nitric acid and then ready to be analyzed.

2.2. Catalyst preparation

2.2.1. Synthesis of $\text{Ni}_x\text{Co}_{2-x}\text{P}$ NPs

Ni_2P NPs were synthesized according to the previous literature.³ 0.1296 g of NiCl_2 (1.0 mmol) was added in a 100-mL double neck round bottom flask containing 3.22 mL (10 mmol) of oleylamine. The solution was combined with 10 mL of 1-octadecene and 2.60 mL (10 mmol) triphenyl phosphite. The mixture was stirred at 120 $^\circ\text{C}$ for 1 h under vacuum to

remove low-boiling-point volatile impurities, moisture, and oxygen. Then, the temperature was reached to 300 °C under a nitrogen atmosphere and held for 2 h with magnetic stirring to give a black colloidal solution. The mixture was then allowed to cool to room temperature, and the black product was isolated by precipitation in acetone. To remove as much organic material as possible, the obtained precipitate was then washed with chloroform–acetone (1:1, v/v) mixed solvent until the supernatant was transparent. The obtained powder was dried at 70 °C in vacuum overnight. Other metal phosphide NPs, NiCoP (0.5:0.5 mmol) NPs and Co₂P NPs, were also obtained following the same procedure as that for Ni₂P NPs.

2.2.2. Preparation of Cr-K10

Cation-exchanged K10-MMT clay catalysts were prepared following the previous published literature¹¹. 2.0 g of the support K10-MMT was added into a 100-mL round bottom flask containing 50 mL aqueous solution of 0.115 mM CrCl₃·6H₂O. The solution was stirred at room temperature for 24 h. Then the catalyst was collected by filtration and washed with deionized water successively to remove remaining free metal salt in the samples. The resulting catalysts were dried under vacuum at 100 °C overnight.

2.2.3. Preparation of Ni_xCo_{2-x}P/Cr-K10

Following the published procedure,³ 22 mg of Ni₂P NPs was dispersed in a 100-mL round bottom flask containing 50 mL of hexane. The solution was sonicated for 1 h. Then, 1.0 g of Cr-K10 was added into the solution under magnetic stirring at room temperature for 6 h. The obtained powder was dried in vacuum overnight to give Ni₂P/Cr-K10 as a gray powder. The same procedure was used to prepare other NiCoP/Cr-K10 and Co₂P/Cr-K10 catalysts. The samples were then analyzed by PXRD, ICP-OES and TEM techniques.

2.3. Synthesis of ionic liquid

The ionic liquids used in this work were synthesized in our laboratory with the variety of salts and long chain hydrocarbons, including N-methylimidazolium chloride ([HMIM]Cl), 1-butyl-3-methylimidazolium chloride ([BMIM]Cl) and N-methylimidazolium bisulfate ([HMIM][HSO₄]). The chemical structures of these ionic liquids were presented in the **Figure 2-1** and their synthesis methods were described below.

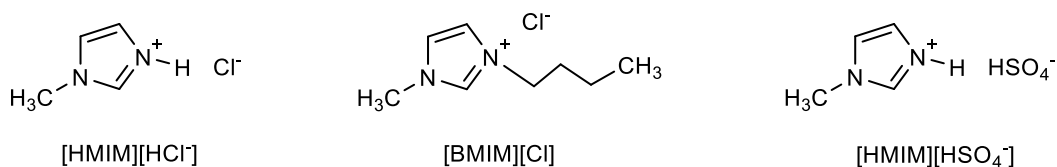


Figure 2-1: Chemical structures of the used ionic liquids.

2.3.1. Synthesis of [HMIM]Cl

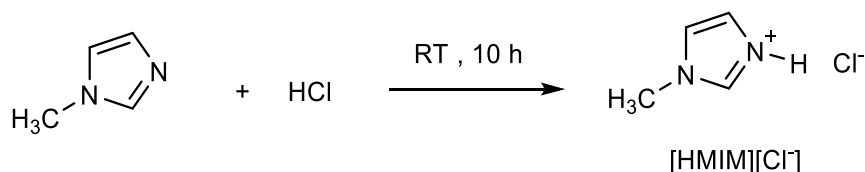


Figure 2-2: Synthesis procedure for [HMIM]Cl.

[HMIM]Cl was prepared according to the previous literature.³³ A 250-mL round bottom flask containing 39.21 mL (approximately 0.497 mol) of N-methylimidazole was cooled in ice bath. 41.73 mL (approximately 0.497 mol) of aqueous solution of HCl (36.5%) was added dropwise into the solution at 0 °C under magnetic stirring. The mixture was stirred at room temperature for 10 h. The resulting solution was then evaporated by rotary evaporation under reduced pressure of about 1 kPa at 65 °C for 2 h and then dried under vacuum overnight. ¹H NMR (500.0 MHz 25 °C, DMSO-d₆): δ (ppm) 9.117 (s, 1H), 7.700 (s, 1H), 7.629 (s, 1H), 3.861 (s, 3H).

2.3.2. Synthesis of [BMIM]Cl

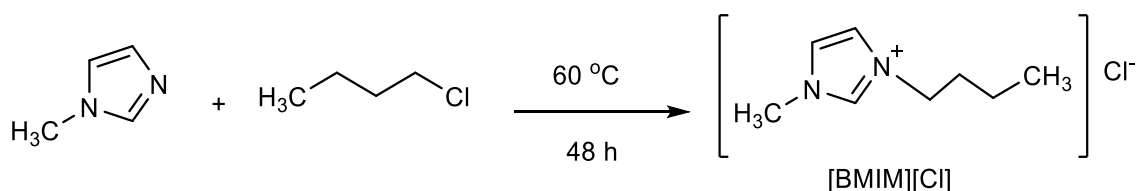


Figure 2-3: Synthesis procedure for [BMIM]Cl.

Following the published procedure,³⁴ [BMIM]Cl was prepared by the reaction of equimolar amounts of N-methylimidazole and 1-chlorobutane. 39.85 mL (0.5 mol) of N-methylimidazole and 52.24 mL (0.5 mol) of 1-chlorobutane was mixed in a 250-mL round bottom flask with magnetic stirring at 60 °C using oil bath under reflux for 48 h and then cooled to room temperature. The resulting solution was washed twice using ethyl acetate.

The remaining ethyl acetate was removed by rotary evaporation under reduced pressure of about 1 kPa at 60 °C for 2 h and dried under vacuum overnight. ^1H NMR (500.0 MHz 25 °C, DMSO- d_6): δ (ppm) 9.474 (s, 1H), 7.862 (s, 1H), 7.788 (s, 1H), 4.189 (t, $J=7.2$ Hz, 2H), 3.868 (s, 3H), 1.723-1.783 (qui, 2H), 1.197-1.271 (sex, 2H), 0.863-0.892 (t, $J=7.2$ Hz, 3H).

2.3.3. Synthesis of [HMIM][HSO₄]

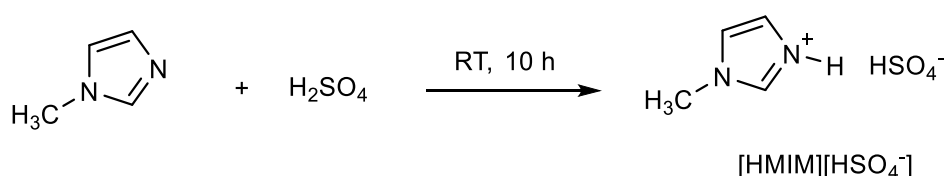


Figure 2-4: Synthesis procedure for [HMIM][HSO₄].

[HMIM][HSO₄] was synthesized following the previous published literature³⁵ by the reaction of N-methylimidazole and H₂SO₄ aqueous solution. 26.63 mL (0.5 mol) of H₂SO₄ aqueous solution was dropwise added into a 250-mL round bottom flask containing 39.48 mL (0.5 mol) of N-methylimidazole in ice bath under magnetic stirring. The mixture was stirred continuously for 10 h at room temperature. The resulting aqueous solution was purified in vacuum oven at 95 °C for 12 h to remove the remaining water. ^1H NMR (400.0 MHz 25 °C, DMSO- d_6): δ (ppm) 9.022 (s, 1H), 7.682 (s, 1H), 7.626 (s, 1H), 3.865 (s, 3H).

2.4. Catalytic reaction procedure

In this study, we firstly focused on the catalytic activity using Cr-K10 catalyst in the variety of ionic liquids, including [HMIM]Cl, [BMIM]Cl and [HMIM][HSO₄] to find an optimal medium for the reaction. Then, the ionic liquid, which provided the best catalytic performance, were used in the further study. A typical reaction procedure for the transformation of glucose and fructose to HMF using Cr-K10, Ni₂P/Cr-K10 and Ni₂P mixed with Cr-K10 catalysts were described below. 50 mg of catalyst was placed in a 3-mL glass vial in an oil bath with magnetic stirring, followed by addition of 50 mg of feedstock and 350 mg of ionic liquid medium. The reaction mixture was stirred vigorously at 120 °C under atmospheric pressure. Samples were collected after 0.5, 1.0, 1.5, 2.0, 2.5 and 3.0 h. Approximately 30 mg of each sample was dissolved in 0.7 mL of DMSO- d_6 and filtered by 0.22 μm syringe filter and then analyzed and calculated HMF yield by ^1H NMR spectroscopy.

Chapter III

Results and Discussion

3.1. Characterizations of catalyst

3.1.1. Characterizations of $\text{Ni}_x\text{Co}_{2-x}\text{P}$ NPs

The crystal structures of the synthesized Ni_2P , NiCoP and Co_2P NPs were confirmed by X-ray diffraction as shown in the **Figure 3-1**. The diffraction peaks of the synthesized Ni_2P and Co_2P NPs (displayed in the **Figure 3-1a** and **3-1b**) were consistent with those of the hexagonal and orthorhombic structure of the Ni_2P and Co_2P crystals, respectively. Although the patterns did not match exactly, but the key peaks could be observed as the broad and low intensity peaks which suggested the formation of nanosized Ni_2P and Co_2P .^{4,14} For the NiCoP sample as demonstrated in the **Figure 3-1c**, major diffraction peaks at $2\theta = 40.8^\circ$, 44.6° , 47.3° , 54.2° and 75.3° were observed and attributed to the (111), (201), (210), (300) and (212) planes, respectively, which could be indexed the same hexagonal structure as Ni_2P .²⁷ Furthermore, the peak positions were more similar to the Ni_2P characteristic peaks, except the first dominant peak around $2\theta = 40-41^\circ$ arising from combination of intensities between Ni_2P and Co_2P . Hence, it was confirmed the successful formation of NiCoP NPs.

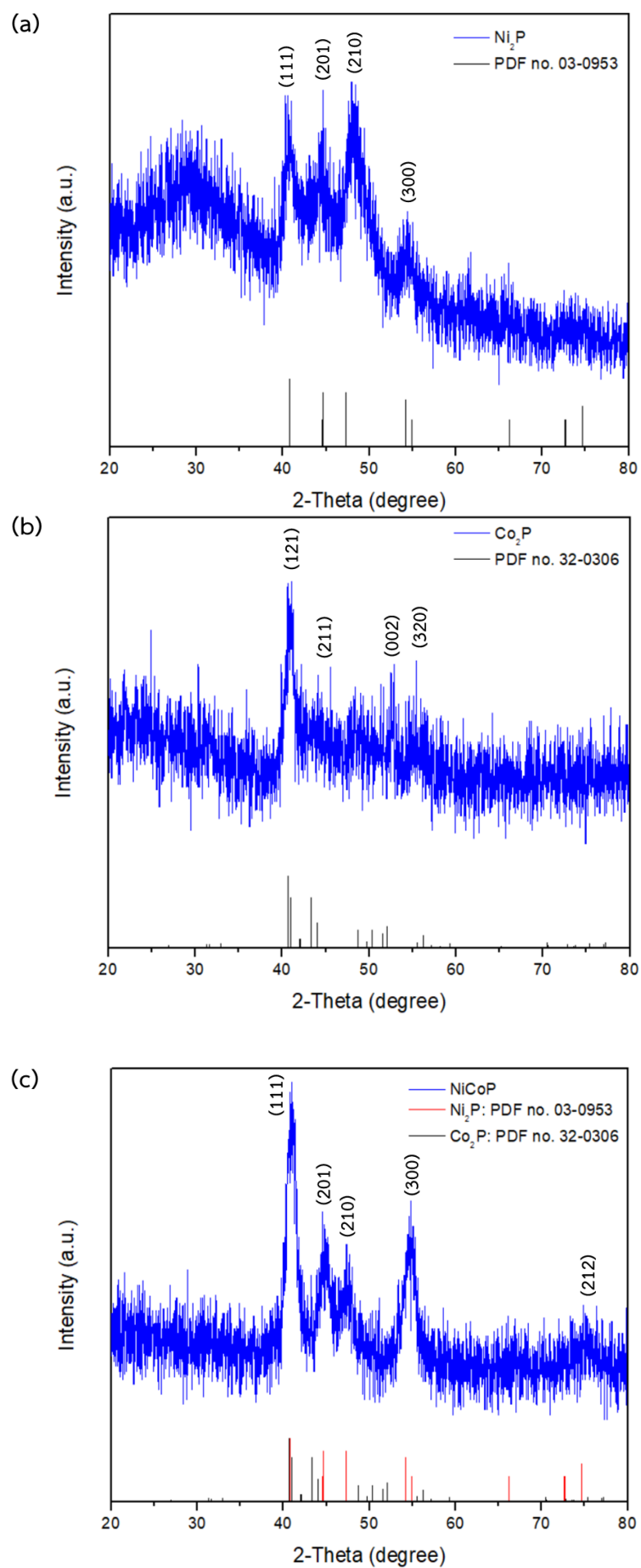


Figure 3-1: XRD patterns of the synthesized (a) Ni_2P (b) Co_2P (c) NiCoP NPs.

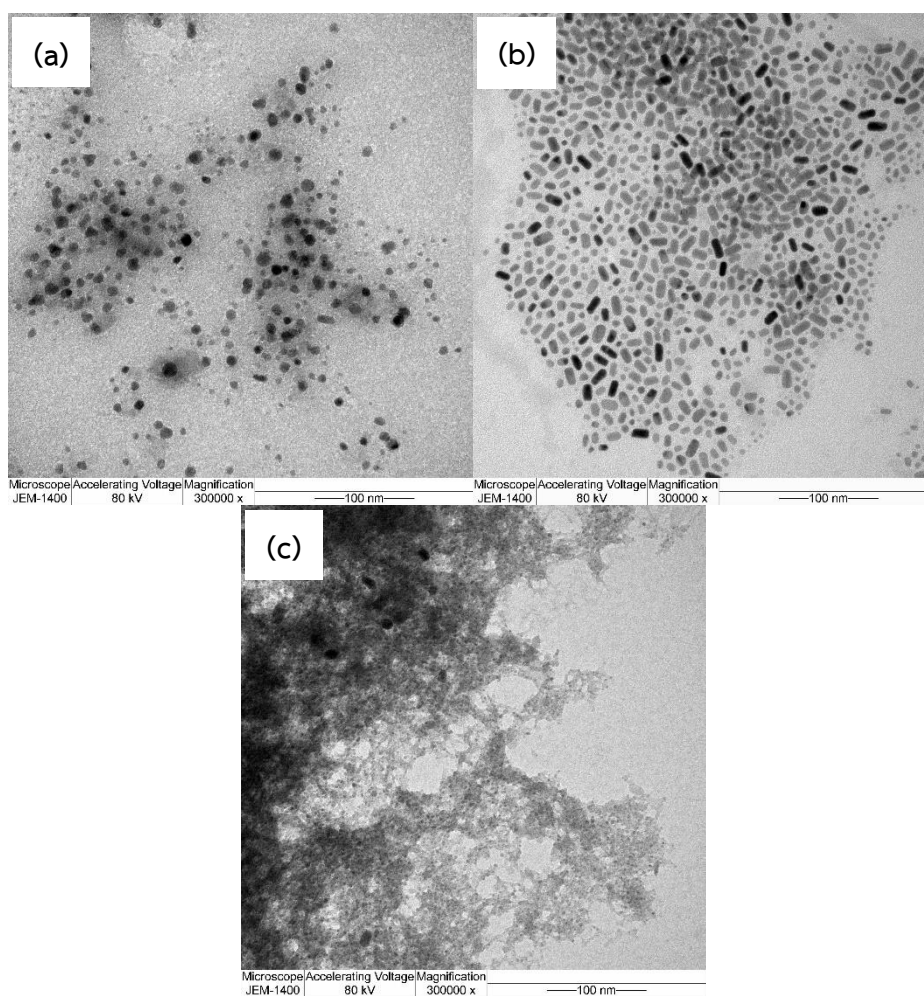


Figure 3-2: TEM images of (a) Ni₂P (b) Co₂P (c) NiCoP NPs.

The representative transmission electron microscopy (TEM) images of the synthesized Ni₂P, NiCoP and Co₂P NPs were captured to determine their morphology and particle size as presented in the **Figure 3-2**. The image of Ni₂P (**Figure 3-2a**) showed that the particle sizes were in the range of 6-15 nm in spherical shape. For the TEM image of Co₂P NPs (**Figure 3-2b**) showed the uniform formation of a nanorod structure with an approximate length of 18 nm and width of 9 nm. Irregular-shape particles were observed in the **Figure 3-2c**. The particle sizes of NiCoP were slightly smaller than those of Ni₂P and Co₂P NPs.

3.1.2. Characterization of Cr-K10

As shown in **Figure 3-2**, the XRD pattern of commercial montmorillonite K10 clay (K10-MMT) and the prepared Cr-K10 showed low crystallinity, and amorphous of clay. The main sharp peak at $2\theta = 26.62^\circ$ was observed in both XRD patterns of K10-MMT and Cr-K10 indicated existence of quartz (SiO₂) mineral, which was consistent with previous literature.³⁶

The diffractogram of the prepared Cr-K10 had the same characteristic peaks as those of K10-MMT but was slightly shifting to the left in second decimal changes. Thus, it referred that inserting Cr metal had no effect on the interlayer of K10-MMT. In addition, it was found that there was no significantly different between the XRD patterns of K10-MMT and the prepared Cr-K10, which indicated that the clay structure was retained after the exchange of Cr metal. However, the change in diffractogram according to Cr-exchanged synthetic process could be observed in low angle below $2\theta = 5$, which is the limitation of instrument.⁹

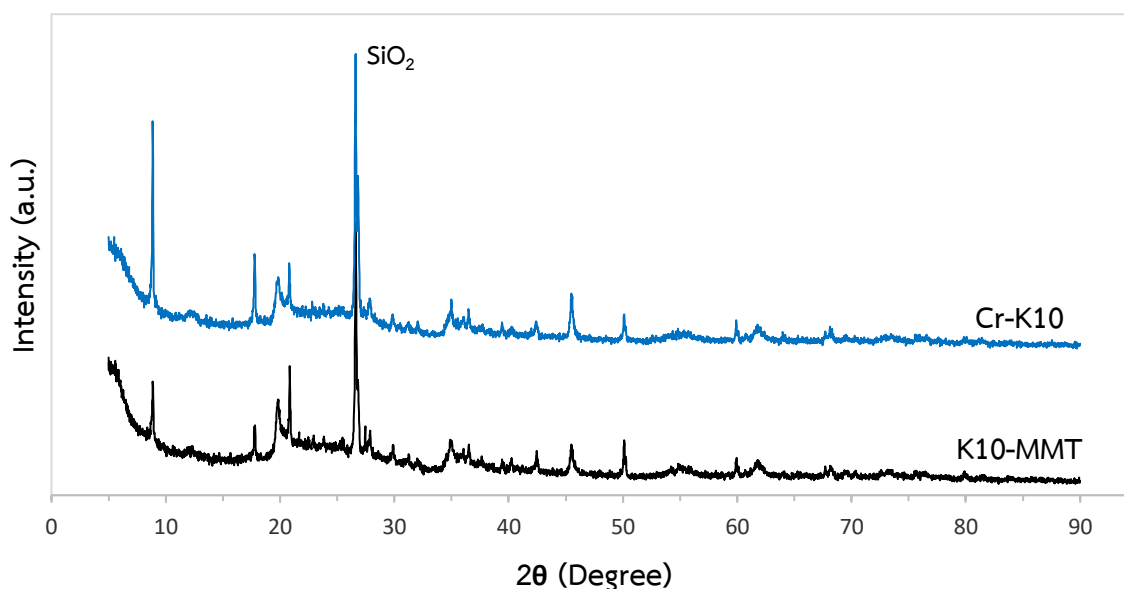


Figure 3-3: XRD patterns of K10-MMT and the prepared Cr-K10.

Figure 3-4 shows FT-IR spectra of K10-MMT and the prepared Cr-K10. After inserting Cr metal into the K10-MMT interlayer, there were little shifting peaks to the higher wavenumber than those of the K10-MMT. The wavenumbers of K10-MMT and the prepared Cr-K10 at 792 and 795 cm^{-1} , respectively, indicate Si-O-Si vibration, because K10-MMT has quartz mineral. The spectra of both clays showed a strong sharp peak at wavenumber 1034 and 1041 cm^{-1} which indicated occurrence absorption of Si-O-Si bending vibration as element composed of K10-MMT. The Cr metal in interlayer was shown at shift wavenumber because they effected of vibrational Si-O-Si bonding groups. It was confirmed by the shift peak at wavenumber 464 to 466 cm^{-1} as well.³⁷ The wavenumber at 530 cm^{-1} of K10-MMT showed existence Si-O-Al bending vibration and the H-OH bond through stretching and bending vibration was shown a broad peak at wave number at 3418 and 1634 cm^{-1} , respectively, indicated that K10-MMT had content of water molecules.

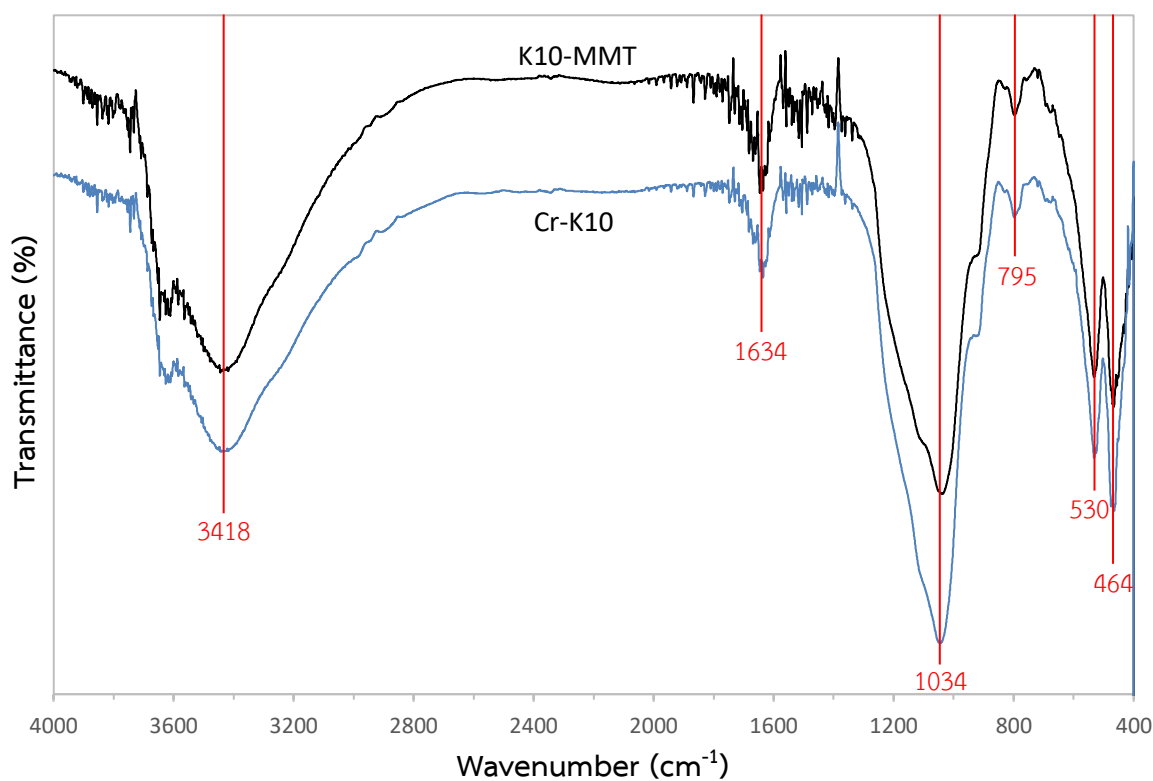


Figure 3-4: FT-IR spectra of K10-MMT and the prepared Cr-K10.

3.1.3. Characterization of $\text{Ni}_x\text{Co}_{2-x}\text{P}/\text{Cr-K10}$

The crystal structures of the synthesized Cr-K10 supported Ni_2P , NiCoP and Co_2P NPs ($\text{Ni}_2\text{P}/\text{Cr-K10}$, $\text{NiCoP}/\text{Cr-K10}$ and $\text{Co}_2\text{P}/\text{Cr-K10}$) were confirmed by X-ray diffraction. As shown in **Figure S4**, the XRD patterns of the entire catalysts represented the patterns that were similar to those of Cr-K10, which were corresponding to characteristic mineral of K10-MMT. As described above, a similar nature in the spectrum of the three catalysts suggested no structural change in the clay matrix and the clay structure was retained after dispersing Ni_2P , NiCoP and Co_2P into the prepared Cr-K10 to obtain $\text{Ni}_2\text{P}/\text{Cr-K10}$, $\text{NiCoP}/\text{Cr-K10}$ and $\text{Co}_2\text{P}/\text{Cr-K10}$, respectively. Therefore, the $\text{Ni}_x\text{Co}_{2-x}\text{P}/\text{support}$ was successfully synthesized. As in the results of FT-IR spectra of the synthesized $\text{Ni}_2\text{P}/\text{Cr-K10}$, $\text{NiCoP}/\text{Cr-K10}$ and $\text{Co}_2\text{P}/\text{Cr-K10}$ (**Figure S5**), the entire samples showed strong characteristic peaks owing to a quartz mineral in the Cr-K10 structure used as support as mentioned in **section 3.1.2**. Because of the dominance of SiO_2 and small amount of Cr ion dispersed on Cr-K10, no Cr ion signal was observed in FT-IR spectrum. As described above, it suggested that there was no structural change in the synthesized $\text{Ni}_2\text{P}/\text{Cr-K10}$, $\text{NiCoP}/\text{Cr-K10}$ and $\text{Co}_2\text{P}/\text{Cr-K10}$, which consistent with XRD results. In

the **Figure 3-5**, it was observed in TEM image that Ni₂P was well dispersing on Cr-K10 support, suggesting that the successful synthesis of Ni₂P/Cr-K10 was confirmed.

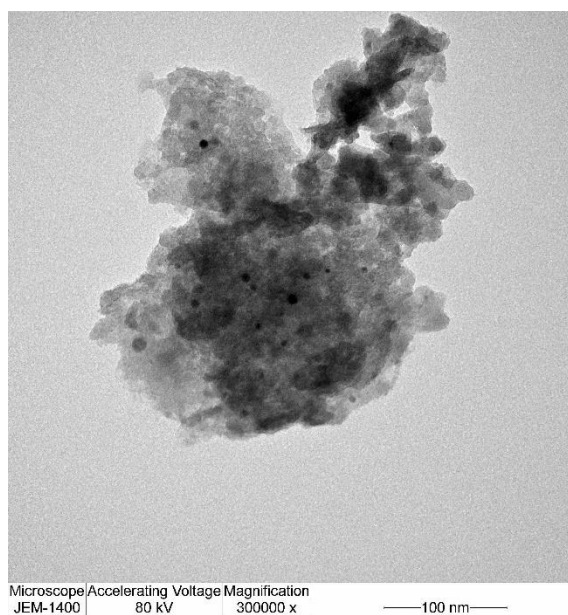


Figure 3-5: TEM images of Ni₂P/Cr-K10.

3.1.4. N₂ adsorption–desorption study

Figure 3-6 shows the N₂ adsorption–desorption isotherms for K10-MMT, the prepared Cr-K10 and Ni₂P/Cr-K10. All the samples behaved according to the same trend. As can be seen from the curve, all of them showed a typical hysteresis loop according to BDDT (Brunauer–Deming–Deming–Teller), suggesting mesoporous materials.³⁸ All the samples were examined by this technique and the main results are summarized as shown in the **Table 3-1**. The specific surface area and pore volume of the prepared Cr-K10 analyzed by BET method were 226.26 m² g⁻¹ and 0.3107 cm³ g⁻¹, respectively, which is rather larger than that of K10-MMT (139.93 m² g⁻¹ and 0.2242 cm³ g⁻¹, respectively) due to additional specific surface area resulting from inserting Cr metal to interlayer of K10-MMT. It was obtained the changes in specific surface area and pore volume of K10-MMT, which indicated additional molecules, that was adsorbed in samples. After the dispersing of Ni₂P NPs onto Cr-K10, a substantial decrease in nitrogen uptake was reflected in a decrease in surface area and pore volume of the Ni₂P/Cr-K10. The specific surface area and pore volume of Ni₂P/Cr-K10 were 212.03 m² g⁻¹ and 0.2989 cm³ g⁻¹, respectively. Such a decrease in these parameters could be attributed to the space occupied by dispersing Ni₂P NPs. While a decrease in the surface area and pore volume was observed, it could also be noted an increase in pore diameter in the Ni₂P/Cr-K10

(5.6394 nm) which was more than the prepared Cr-K10 (5.4929 nm). A considerable decrease in the BET surface area and pore volume and an increase in pore diameter of Ni₂P/Cr-K10 suggested the possibility that the Ni₂P NPs might had been anchored on the interlayer of the mesopores.

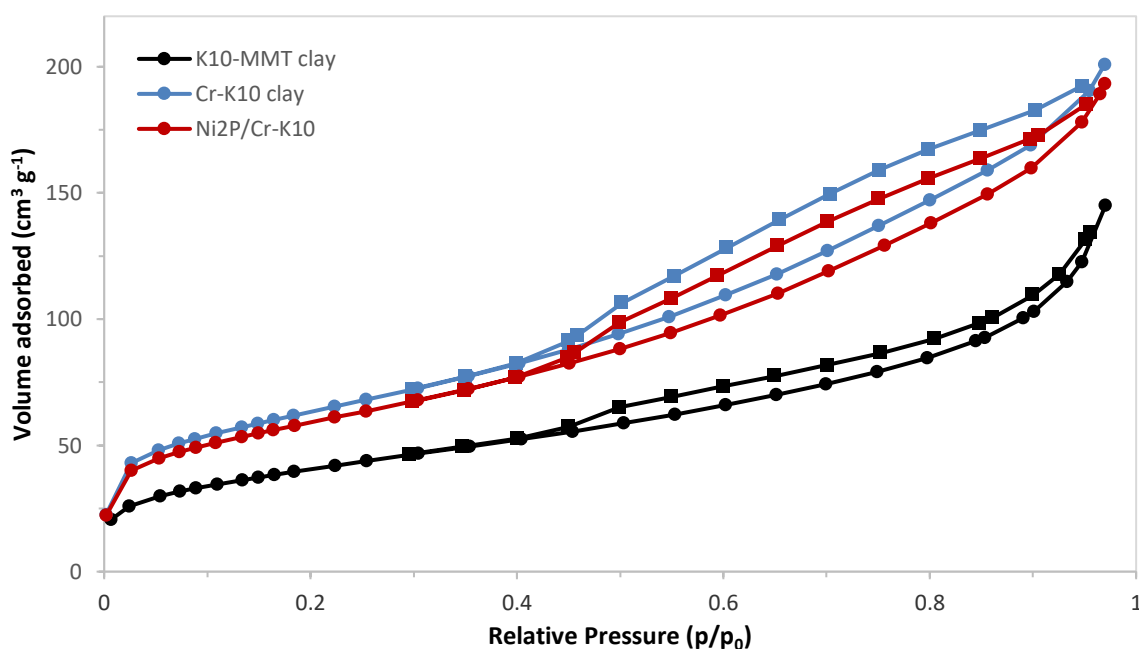


Figure 3-6: The N₂ adsorption–desorption isotherms spectra of K10-MMT, the prepared Cr-K10 and the synthesized Ni₂P/Cr-K10.

Table 3-1: Surface properties of K10-MMT, the prepared Cr-K10 and the synthesized Ni₂P/Cr-K10.

Catalyst	Specific surface area (m ² g ⁻¹)	Pore volume (cm ³ g ⁻¹)	Pore diameter (nm)
K10-MMT	139.93	0.22	6.4
Cr-K10	226.26	0.31	5.5
Ni ₂ P/Cr-K10	212.03	0.30	5.6

3.1.5. Elemental composition study

Because chromium and nickel possessed Lewis acid property that were beneficial for the catalytic conversion of glucose and fructose into HMF. Therefore, it became an important issue that amount of chromium and nickel in the synthesized Ni₂P/Cr-K10 catalyst should be investigated. ICP-OES was used to determine the chemical composition of the synthesized

materials. The results of chromium and nickel elemental analysis of the prepared materials suggested that chromium and nickel were loaded onto the synthesized Ni₂P/Cr-K10 catalyst at 0.0983 and 0.1401 mmol g⁻¹ of catalyst, respectively, as demonstrated in the **Table 3-2**. The presence of chromium and nickel in the synthesized Ni₂P/Cr-K10 catalyst suggested that Ni₂P NPs were successfully dispersed on Cr-K10.

Table 3-2: The elemental analysis of the synthesized Cr-K10, Ni₂P NPs and Ni₂P/Cr-K10 determined by ICP-OES.

Catalyst	Elemental content (mmol g ⁻¹)	
	Cr	Ni
Cr-K10	0.0753	-
Ni ₂ P NPs	-	0.0532
Ni ₂ P/Cr-K10	0.0983	0.1401

3.2. Characterization of ionic liquids

Successful synthesis of ionic liquids, including [HMIM]Cl, [BMIM]Cl and [HMIM][HSO₄], was confirmed by ¹H NMR spectroscopy. **Figure 3-7** demonstrated the resonances of each proton position of all ionic liquids. The resonances at the δ 9.117 (a, s, 1H), 7.700 (b, s, 1H) and 7.629 (c, s, 1H) ppm belonged to the protons in an aromatic imidazole ring of [HMIM]Cl and the methyl proton appeared at the δ 3.861 (d, s, 3H) ppm as shown in **Figure 3-7a**. The ¹H NMR spectrum of [HMIM][HSO₄] (**Figure 3-7c**) was similar to that of [HMIM]Cl which illustrated only four different types of protons. The resonances which appeared at the δ 9.022 (a, s, 1H), 7.682 (b, s, 1H) and 7.626 (c, s, 1H) ppm were possessed by the protons in an aromatic imidazole ring of [HMIM][HSO₄], as same as the methyl proton which was observed at δ 3.865 (d, s, 3H) ppm. ¹H NMR data of [BMIM]Cl was corresponding to the protons in [BMIM]Cl structure. The resonances at the δ 9.474 (a, s, 1H), 7.862 (b, s, 1H) and 7.788 (c, s, 1H) ppm belonged to the protons in an aromatic imidazole ring of [BMIM]Cl and the methyl proton connected with the imidazole ring appeared at the δ 3.868 (e, s, 3H) ppm. The left n-butyl protons were fully characterized as labeled in the **Figure 3-7b**. It was found that there were a lot of peaks of impurities in the synthesized [BMIM]Cl. So, the predictions with those were the remaining of 1-chlorobutane and ethyl acetate which were a substrate and a solvent used for washing, respectively.

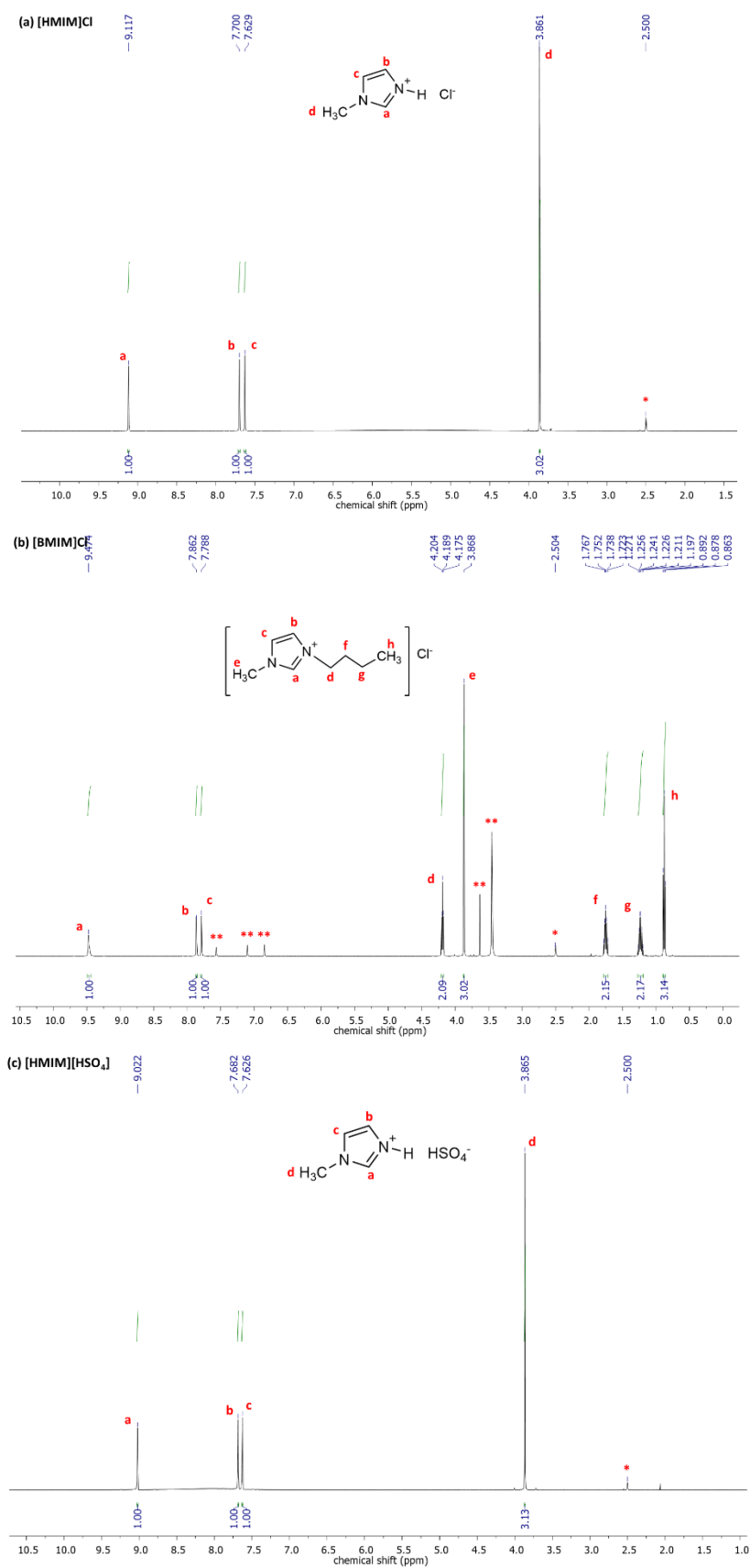


Figure 3-7: ^1H NMR spectra (500.0 MHz 25 °C, DMSO-d_6) of the synthesized (a) [HMIM]Cl (b) [BMIM]Cl (c) [HMIM][HSO_4]. An asterisk (* and **) signifies the DMSO-d_6 and impurities, respectively.

Aside from ^1H NMR spectra of all ionic liquids, they were also measured by FT-IR analysis. As shown in the **Figure 3-8**, the FT-IR spectrum of [HMIM]Cl showed the peaks at wavenumber 2968 and 2856 cm^{-1} which were the aliphatic C-H stretching vibration due to methyl group connected the aromatic imidazole ring. A broad peak in the range 3340-3460 cm^{-1} belonged to the quaternary amine salt formation with chloride. The peaks which appeared at wavenumber 3067, 1633 and 1084 cm^{-1} were due to the =C-H stretching, C=N stretching vibration of the aromatic imidazole ring and C-N stretching vibration, respectively. As in FT-IR spectrum of [BMIM]Cl, the peaks showed at wavenumber 2958 and 2872 cm^{-1} belonged to C-H stretching vibration due to the alkyl group in [BMIM]Cl structure. The formation of quaternary amine salt formation with chloride was showed in a broad peak in a range of 3330-3470 cm^{-1} . The wavenumbers at 3073, 1638 and 1164 cm^{-1} were indicated of the =C-H stretching, C=N stretching vibration of the aromatic imidazole ring and C-N stretching vibration, respectively. The very broad peak in a range of 2420-3600 cm^{-1} belonged to N-H stretching vibration which suggested the formation of quaternary amine salt with hydrogen sulphate in [HMIM][HSO₄] structure. The others peaks appeared at wavenumber 1631 and 1047 cm^{-1} were indicated of the C=N stretching vibration of the aromatic imidazole ring and C-N stretching vibration, respectively. Based on ^1H NMR spectra and FT-IR analysis, it was observed that the synthesis of all ionic liquids was successful.

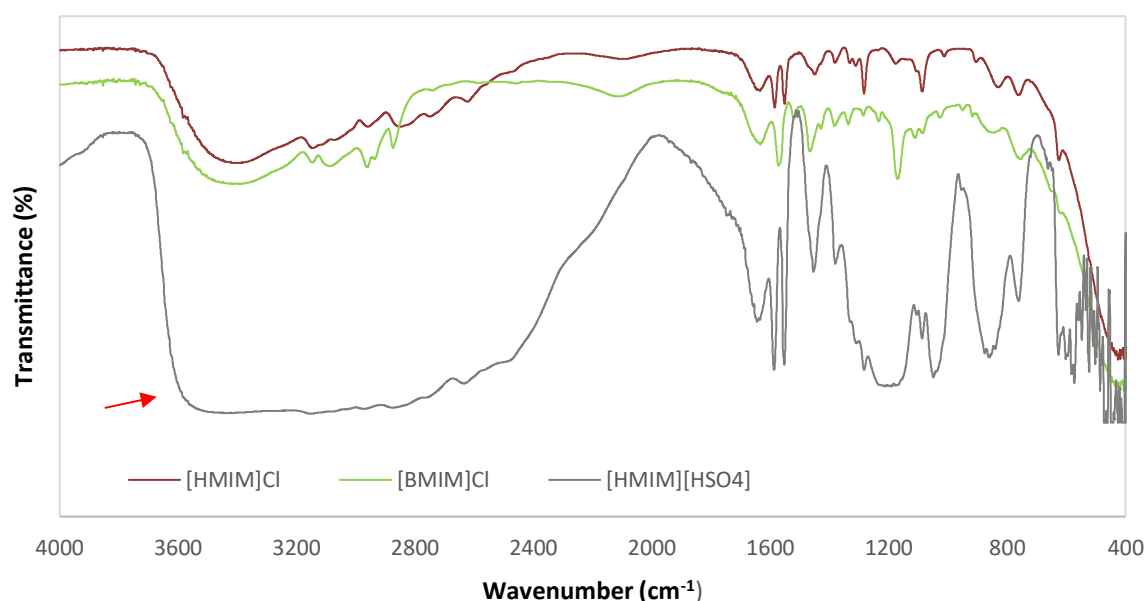
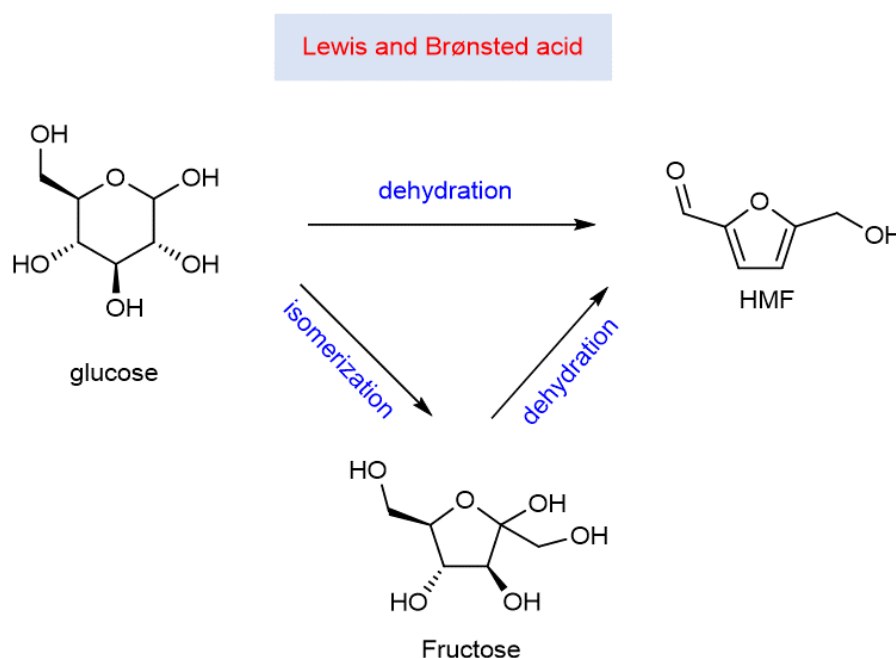


Figure 3-8: FT-IR spectra of the synthesized [HMIM]Cl, [BMIM]Cl and [HMIM][HSO₄].

3.3. The catalytic studies towards sugar conversion to HMF

The supported nickel phosphide catalyst used for hydrolytic hydrogenation exhibited bifunctionality through the Brønsted and Lewis acid sites on the support (Cr-K10) and the nickel sites in nickel phosphides. Due to the limit of time, we focus on only the catalytic activity in the first dehydration part using Cr-K10 that catalyzed the conversion of sugar to HMF in this study since the first reaction was bottle neck reaction for the two-step tandem reaction. The studied catalytic mechanism could be summarized as shown in **Scheme 3-1**.



Scheme 3-1: Glucose and fructose conversion to HMF.

3.3.1. Determination of optimal ionic liquid media for glucose conversion

To investigate the effects of the different ionic liquids on the conversion of glucose, three kinds of ionic liquids, including [HMIM]Cl, [BMIM]Cl and [HMIM][HSO₄], were examined with the prepared Cr-K10 as catalyst. An experiment to modulate the ionic liquid medium was carried out as presented in the **Figure 3-9**. After the reaction under mild condition (at 120 °C for 1 h), the satisfied yield of produced HMF was obtained in the [HMIM]Cl medium as shown in the **Figure 3-9b**. It strongly suggested that Cr-K10 possessed a stable catalytic activity on dehydration of glucose to HMF in [HMIM]Cl the most, and no trace amounts of the products from side reactions such as levulinic acid, formic acid and/or humin were observed. With [HMIM][HSO₄] and [BMIM]Cl as the media, Cr-K10 showed a poor catalytic

activity, which may be attributed to the lower solubility of the glucose. From this observation of low produced HMF in [HMIM][HSO₄], it was clear that the Lewis basic ionic liquid (containing the Cl⁻ anion) was more suitable than the Brønsted acidic solvent ([HSO₄]⁻ anion). This was likely to be due to the formation of [CrCl₄]⁻ in solution from the Cr ions in Cr-K10 support, which was capable of promoting the glucose conversion. In contrast, the [HSO₄]⁻ ion could not form such a complex.¹² Therefore, it was probably less able to catalyze the glucose conversion, resulting in very low HMF products. Therefore, [HMIM]Cl was chosen as the optimum candidate in further experiment.

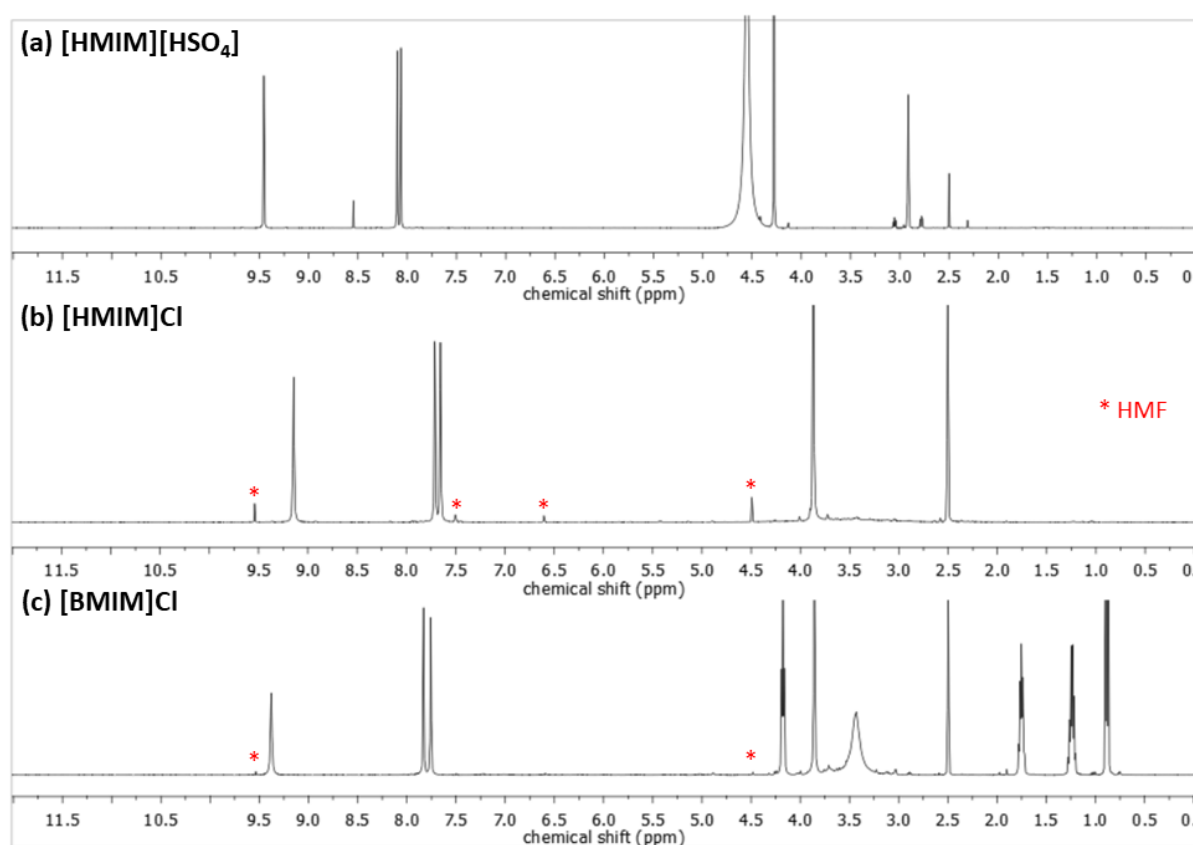


Figure 3-9: Stacked ¹H NMR spectra (500.0 MHz 25 °C, DMSO-d₆) of glucose conversion for 1 h using Cr-K10 catalyst in (a) [HMIM][HSO₄] (b) [HMIM]Cl (c) [BMIM]Cl as media.

3.3.2. Conversion of glucose and fructose to HMF using Cr-K10 as catalyst

Once the variation of ionic liquids had been investigated, additional data were collected to examine the effect of longer reaction times on the conversion of glucose and fructose to HMF. The effect of reaction time on the efficiency of the dehydration of glucose was assessed at 120 °C in the presence of Cr-K10 catalyst using [HMIM]Cl, the best-performing ionic liquid from the previous section, as the representative medium. It was hoped that this

would help elucidate whether the low yield was only due to slow kinetics, or if HMF side reactions (to form levulinic acid, formic acid and/or humins) would occur over extended reaction times. Low amount of HMF (13%) was detected over the period of reaction. If the ^1H NMR spectra were closely speculated (**Figure S4**), the broad baseline-resonance around 2.75-4.25 ppm may suggest the presence of other side products, of which their ^1H NMR spectra were supplemented in appendix.

The more facile conversion of fructose was attempted. Fructose behavior was then studied to compare the catalytic activity towards sugar conversion into HMF in the same condition due to the findings reported that glucose could transform to fructose by isomerization. Around 50% was detected in the first 0.5 h and the maximum conversion around over 60% was reached in the first hour and remained unchanged over the period of investigation within errors. When the yield of HMF was calculated from these two figures as summarized in the **Table 3-3**, the HMF yields of both of them were obtained and increasing when the reaction continued. However, the yield of HMF from fructose conversion dropped over longer reaction times after 2 h. In addition, it was found that HMF product was produced very little from glucose compared with the yield from fructose conversion, presumably due to the ease of cleaving the furanose ring of fructose relative to the pyranose ring of glucose. Another possible explanation is that fructose may be an intermediate in the conversion of glucose into furfural through the transformation,³⁹ the isomerization of glucose to fructose as illustrated in **Scheme 3-1**. From those results, it suggested that the prepared Cr-K10 could be used to catalyze the conversion of sugar into HMF because of its Brønsted and Lewis acid active sites in Cr-K10.

Table 3-3: Yield of HMF from glucose and fructose conversion using Cr-K10 catalyst in [HMIM]Cl medium at different reaction time.^a

Entry	Catalyst	Feedstock	HMF yield (%) for					
			0.5 h	1.0 h	1.5 h	2.0 h	2.5 h	3.0 h
1	Cr-K10	glucose	1	4	6	8	9	13
2	Cr-K10	fructose	49	62	65	64	64	61

^a Reaction condition: 50 mg feedstock, 50 mg catalyst, 350 mg of [HMIM]Cl medium, 120 °C.

3.3.3. Conversion of glucose and fructose to HMF using Ni₂P/Cr-K10 as catalyst

To compare the performance of the Ni₂P/Cr-K10 catalyst with the Cr-K10 catalyst, the catalytic activity of the Ni₂P/Cr-K10 catalyst in the glucose and fructose dehydration reaction in [HMIM]Cl medium at 120 °C under different reaction times was shown in the **Figure S8** and **Figure S9**, respectively. It was observed that both ¹H NMR spectra of the product using Ni₂P/Cr-K10 and Cr-K10 were appeared similarly. In the glucose conversion, low HMF yield were emerged in ¹H NMR spectrum, and also the broad baseline-resonance around 2.75-4.25 ppm, that indicated traces of the side reaction products such as levulinic acid, formic acid and/or humins. As in the fructose dehydration reaction, it confirmed the formation of HMF from the ¹H NMR spectrum as the main product. It suggested that these two catalysts, Ni₂P/Cr-K10 and Cr-K10, resulted in being more considerably selective to the dehydration reaction of fructose to HMF than glucose due to the reasons mentioned above in the previous section. The produced HMF yield was then calculated and summarized in the **Table 3-4**.

Table 3-4: Yield of HMF from glucose and fructose conversion using Ni₂P/Cr-K10 catalyst in [HMIM]Cl medium at different reaction time.^a

Entry	Catalyst	Feedstock	HMF yield (%) for					
			0.5 h	1.0 h	1.5 h	2.0 h	2.5 h	3.0 h
1	Ni ₂ P/Cr-K10	glucose	1	2	3	5	7	6
2	Ni ₂ P/Cr-K10	fructose	64	67	68	67	57	53

^a Reaction condition: 50 mg feedstock, 50 mg catalyst, 350 mg of [HMIM]Cl medium, 120 °C.

It was found that the yield of produced HMF using Ni₂P/Cr-K10 catalyst behaved according to the same trend as well as Cr-K10 catalyst. For the glucose conversion, a gradual increase in the yield of HMF was observed with increasing reaction time up to 2.5 h and was slowly decreased after 2.5 h. As for the HMF yield form dehydration of fructose, it increased to the yield of 68% at the initial 1.5 h. With the reaction time prolonged to 3 h, the yield of HMF declined a lot with the decomposition of unstable HMF and the formation of other products from side reactions, levulinic acid and humins, as mentioned in the previous section. From those results, it suggested that the presence of Ni₂P in Cr-K10 did not reduce the catalytic performance and hinder the reaction towards sugar conversion into HFM.

3.3.4. Conversion of glucose and fructose to HMF using Ni₂P mixed with Cr-K10

Since Cr³⁺ in Cr-K10 might be replaced by Ni₂P NPs during the preparation of Ni₂P/Cr-K10 resulting in the decrease in catalytic activity. Therefore, to prove this possibility, the conversion reaction of glucose and fructose using Ni₂P mixed with Cr-K10 was studied. The produced product from glucose and fructose was displayed in the **Figure S10** and **S11**. The percent yield of HMF was calculated by ¹H NMR integration and listed in the **Table 3-5**. It was observed that the results of HMF yield from glucose using the Ni₂P mixed with Cr-K10 catalyst were slightly higher than those when using Cr-K10 and Ni₂P/Cr-K10 catalyst. For the result of fructose conversion, the yield of HMF reached to the yield of 69% at the initial 0.5 h of reaction time and then considerably decreased as the reaction time increased. When compared the HMF yield from the previous section, it was observed that the HMF yield was not significantly different from those results of Ni₂P/Cr-K10 catalyst. These suggested that Ni₂P NPs did not replace the chromium ion which resided in Cr-K10 during the preparation of Ni₂P/Cr-K10.

Table 3-5: Yield of HMF from glucose and fructose conversion using Ni₂P mixed with Cr-K10 catalyst in [HMIM]Cl medium at different reaction time.^a

Entry	Catalyst	Feedstock	HMF yield (%) for					
			0.5 h	1.0 h	1.5 h	2.0 h	2.5 h	3.0 h
1	Ni ₂ P + Cr-K10 mixture	glucose	4	5	6	8	9	9
2	Ni ₂ P + Cr-K10 mixture	fructose	69	59	60	53	52	52

^a Reaction condition: 50 mg feedstock, 50 mg catalyst, 350 mg of [HMIM]Cl medium, 120 °C.

Chapter IV

Conclusions

In this study, we have reported a catalytic system, Cr-exchanged K10-MMT supported metal phosphide nanoparticles ($\text{Ni}_x\text{Co}_{2-x}\text{P}/\text{Cr-K10}$), for the synthesis of HMF from monosaccharides. All catalysts were successfully synthesized by a two-step procedure; the synthesis of metal phosphide nanoparticles and the nanoparticle dispersion on to Cr-exchanged K10-MMT clay. Thorough characterization was carried out using XRD, TEM, FTIR, ICP-OES and BET surface area analyzer. Besides, the effect of ionic liquids, including [HMIM]Cl, [BMIM]Cl and [HMIM][HSO₄], as a catalytic medium in the conversion of monosaccharides to HMF was investigated. Results demonstrated that using [HMIM]Cl provided the highest HMF yield compared to other ionic liquids. For this reason, [HMIM]Cl was used as medium in further catalytic experiment.

The catalytic conversion of two sugars (glucose and fructose) in [HMIM]Cl catalyzed by various catalysts including Cr-K10, $\text{Ni}_2\text{P}/\text{Cr-K10}$ and Ni_2P mixed with Cr-K10 was investigated. HMF yield over 60% was obtained in a short time at 120 °C within 1.5 h when fructose was used as feedstock due to the ease of cleaving the furanose ring of fructose relative to the pyranose ring of glucose. These results suggested that the developed methods were also effective for the synthesis of HMF from fructose and the synthesized $\text{Ni}_2\text{P}/\text{Cr-K10}$ can be potentially applicable for further reductive conversion to other value-added chemicals.

References

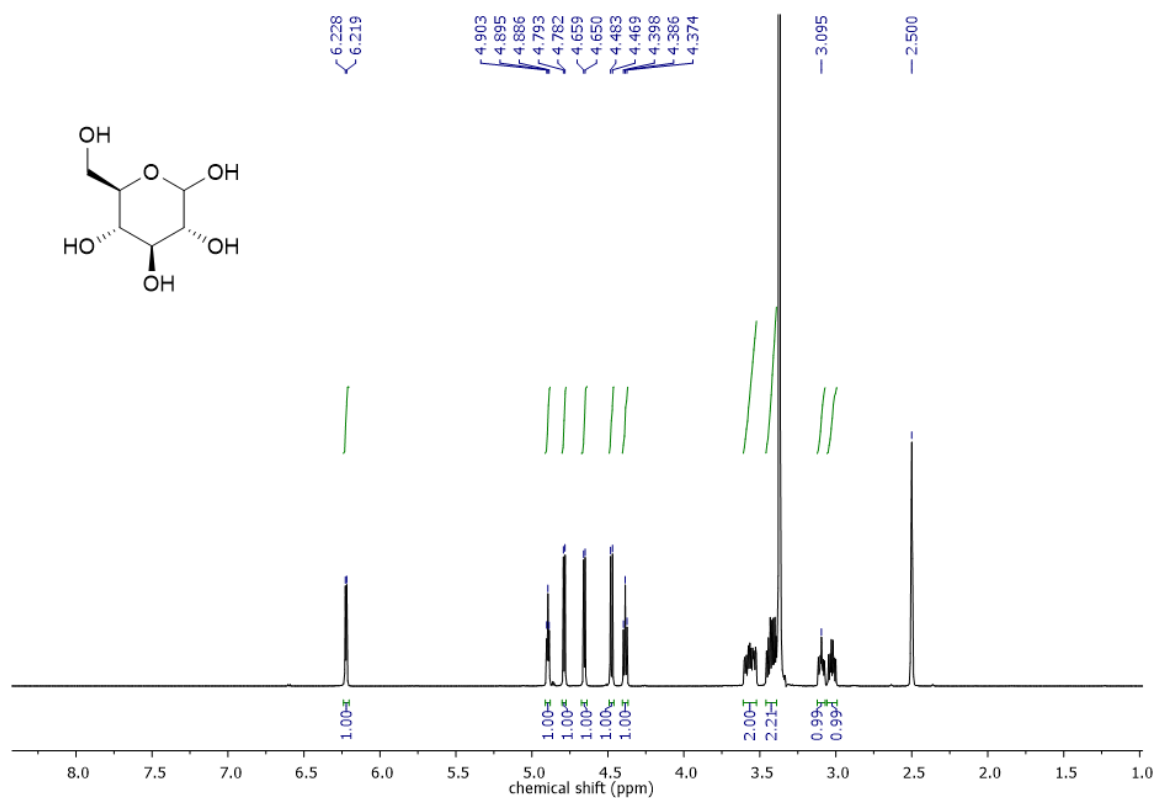
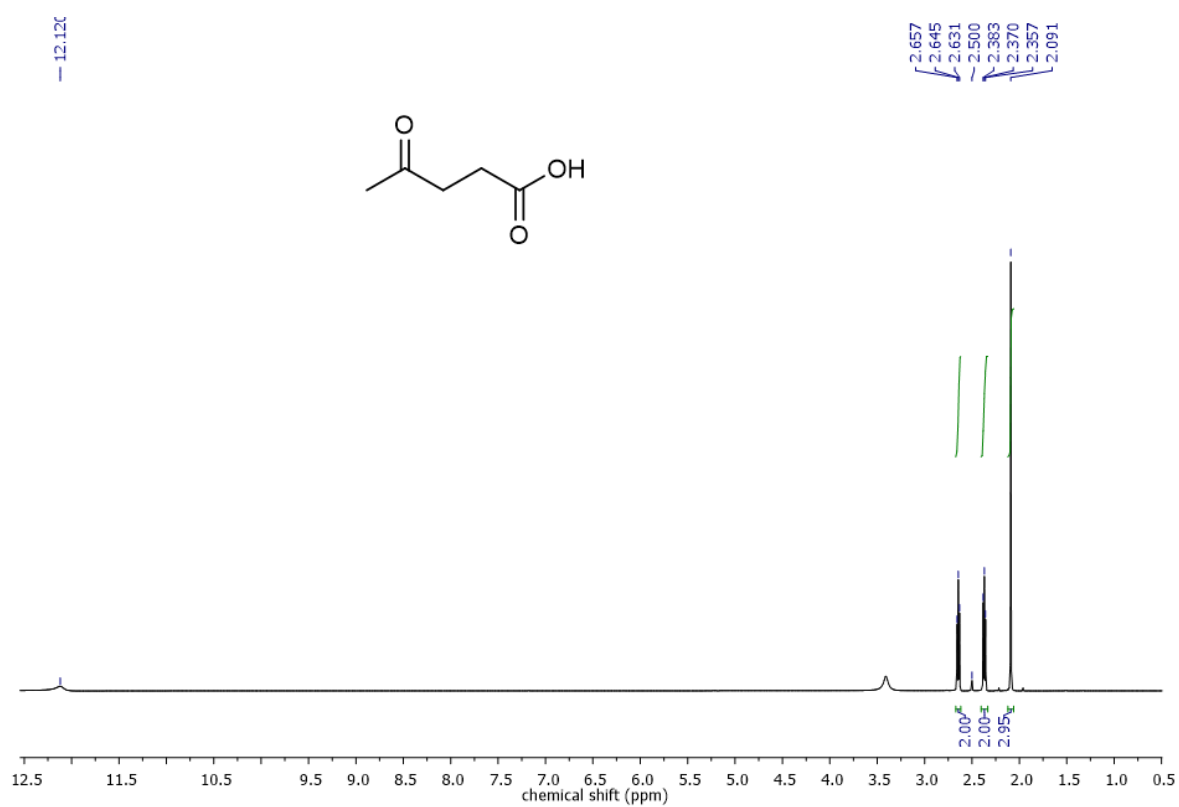
1. Hou, Q.; Qi, X.; Zhen, M.; Qian, H.; Nie, Y.; Bai, C.; Zhang, S.; Bai, X.; Ju, M., Biorefinery roadmap based on catalytic production and upgrading 5-hydroxymethylfurfural. *Green Chemistry* **2021**, *23* (1), 119-231.
2. Zhu, C.; Wang, H.; Cai, C.; Bi, K.; Cai, B.; Song, X.; Liu, Q.; Ma, L., Tandem Conversion of Fructose to 2,5-Dimethylfuran with the Aid of Ionic Liquids. *ACS Sustainable Chemistry & Engineering* **2019**, *7* (19), 16026-16040.
3. Fujita, S.; Nakajima, K.; Yamasaki, J.; Mizugaki, T.; Jitsukawa, K.; Mitsudome, T., Unique Catalysis of Nickel Phosphide Nanoparticles to Promote the Selective Transformation of Biofuranic Aldehydes into Diketones in Water. *ACS Catalysis* **2020**, *10* (7), 4261-4267.
4. Ishikawa, H.; Sheng, M.; Nakata, A.; Nakajima, K.; Yamazoe, S.; Yamasaki, J.; Yamaguchi, S.; Mizugaki, T.; Mitsudome, T., Air-Stable and Reusable Cobalt Phosphide Nanoalloy Catalyst for Selective Hydrogenation of Furfural Derivatives. *ACS Catalysis* **2021**, *11* (2), 750-757.
5. Pagán-Torres, Y. J.; Wang, T.; Gallo, J. M. R.; Shanks, B. H.; Dumesic, J. A., Production of 5-Hydroxymethylfurfural from Glucose Using a Combination of Lewis and Brønsted Acid Catalysts in Water in a Biphasic Reactor with an Alkylphenol Solvent. *ACS Catalysis* **2012**, *2* (6), 930-934.
6. Li, K.; Du, M.; Ji, P., Multifunctional Tin-Based Heterogeneous Catalyst for Catalytic Conversion of Glucose to 5-Hydroxymethylfurfural. *ACS Sustainable Chemistry & Engineering* **2018**, *6* (4), 5636-5644.
7. Tang, Z.; Su, J., One Step Conversion of Glucose into 5-Hydroxymethylfurfural (HMF) via a Basic Catalyst in Mixed Solvent Systems of Ionic Liquid-Dimethyl Sulfoxide. *Journal of Oleo Science* **2019**, *68* (3), 261-271.
8. Cao, J.; Ma, M.; Liu, J.; Yang, Y.; Liu, H.; Xu, X.; Huang, J.; Yue, H.; Tian, G.; Feng, S., Highly effective transformation of carbohydrates to 5-Hydroxymethylfurfural with Al-montmorillonite as catalyst. *Applied Catalysis A: General* **2019**, *571*, 96-101.
9. Qiu, G.; Huang, C.; Sun, X.; Chen, B., Highly active niobium-loaded montmorillonite catalysts for the production of 5-hydroxymethylfurfural from glucose. *Green Chemistry* **2019**, *21* (14), 3930-3939.
10. Varadwaj, G. B. B.; Parida, K. M., Montmorillonite supported metal nanoparticles: an update on syntheses and applications. *RSC Advances* **2013**, *3* (33), 13583-13593.

11. Fang, Z.; Liu, B.; Luo, J.; Ren, Y.; Zhang, Z., Efficient conversion of carbohydrates into 5-hydroxymethylfurfural catalyzed by the chromium-exchanged montmorillonite K-10 clay. *Biomass and Bioenergy* **2014**, *60*, 171-177.
12. Eminov, S.; Brandt, A.; Wilton-Ely, J. D. E. T.; Hallett, J. P., The Highly Selective and Near-Quantitative Conversion of Glucose to 5-Hydroxymethylfurfural Using Ionic Liquids. *PLOS ONE* **2016**, *11* (10), e0163835.
13. Zhang, Z.; Song, J.; Han, B., Catalytic Transformation of Lignocellulose into Chemicals and Fuel Products in Ionic Liquids. *Chemical Reviews* **2017**, *117* (10), 6834-6880.
14. Yamaguchi, S.; Fujita, S.; Nakajima, K.; Yamazoe, S.; Yamasaki, J.; Mizugaki, T.; Mitsudome, T., Air-stable and reusable nickel phosphide nanoparticle catalyst for the highly selective hydrogenation of d-glucose to d-sorbitol. *Green Chemistry* **2021**, *23* (5), 2010-2016.
15. Mei, Q.; Shen, X.; Liu, H.; Liu, H.; Xiang, J.; Han, B., Selective utilization of methoxy groups in lignin for N-methylation reaction of anilines. *Chemical Science* **2019**, *10* (4), 1082-1088.
16. Chen, S.; Wojcieszak, R.; Dumeignil, F.; Marceau, E.; Royer, S., How Catalysts and Experimental Conditions Determine the Selective Hydroconversion of Furfural and 5-Hydroxymethylfurfural. *Chemical Reviews* **2018**, *118* (22), 11023-11117.
17. Mika, L. T.; Cséfalvay, E.; Németh, Á., Catalytic Conversion of Carbohydrates to Initial Platform Chemicals: Chemistry and Sustainability. *Chemical Reviews* **2018**, *118* (2), 505-613.
18. Vaccari, A., Preparation and catalytic properties of cationic and anionic clays. *Catalysis Today* **1998**, *41* (1), 53-71.
19. Pinnavaia, T. J., Intercalated Clay Catalysts. *Science* **1983**, *220* (4595), 365-371.
20. Laszlo, P., Catalysis of organic reactions by inorganic solids. *Accounts of Chemical Research* **1986**, *19* (4), 121-127.
21. Shimizu, K.-i.; Higuchi, T.; Takasugi, E.; Hatamachi, T.; Kodama, T.; Satsuma, A., Characterization of Lewis acidity of cation-exchanged montmorillonite K-10 clay as effective heterogeneous catalyst for acetylation of alcohol. *Journal of Molecular Catalysis A: Chemical* **2008**, *284* (1), 89-96.
22. Aylak, A. R.; Akmaz, S.; Koc, S. N., Glucose conversion to 5-hydroxymethylfurfural with chromium exchanged bentonite and montmorillonite catalysts in different solvents. *Chemical Engineering Communications* **2020**, *207* (8), 1103-1113.
23. Souza, D. C. S.; Pralong, V.; Jacobson, A. J.; Nazar, L. F., A Reversible Solid-State Crystalline Transformation in a Metal Phosphide Induced by Redox Chemistry. *Science* **2002**, *296* (5575), 2012-2015.

24. Xie, R.; Battaglia, D.; Peng, X., Colloidal InP Nanocrystals as Efficient Emitters Covering Blue to Near-Infrared. *Journal of the American Chemical Society* **2007**, *129* (50), 15432-15433.
25. Brock, S. L.; Perera, S. C.; Stamm, K. L., Chemical routes for production of transition-metal phosphides on the nanoscale: implications for advanced magnetic and catalytic materials. *Chemistry* **2004**, *10* (14), 3364-71.
26. Prins, R.; Bussell, M. E., Metal Phosphides: Preparation, Characterization and Catalytic Reactivity. *Catalysis Letters* **2012**, *142* (12), 1413-1436.
27. Sun, L.; Xiang, X.; Wu, J.; Cai, C.; Ao, D.; Luo, J.; Tian, C.; Zu, X., Bi-Metal Phosphide NiCoP: An Enhanced Catalyst for the Reduction of 4-Nitrophenol. *Nanomaterials* **2019**, *9* (1), 112.
28. Liyanage, D. R.; Danforth, S. J.; Liu, Y.; Bussell, M. E.; Brock, S. L., Simultaneous Control of Composition, Size, and Morphology in Discrete Ni_{2-x}CoxP Nanoparticles. *Chemistry of Materials* **2015**, *27* (12), 4349-4357.
29. Mou, J.; Gao, Y.; Wang, J.; Ma, J.; Ren, H., Hydrogen evolution reaction activity related to the facet-dependent electrocatalytic performance of NiCoP from first principles. *RSC Advances* **2019**, *9* (21), 11755-11761.
30. de los Ríos, A. P.; Irabien, A.; Hollmann, F.; Fernández, F. J. H., Ionic Liquids: Green Solvents for Chemical Processing. *Journal of Chemistry* **2013**, *2013*, 402172.
31. Zhao, H.; Holladay, J. E.; Brown, H.; Zhang, Z. C., Metal Chlorides in Ionic Liquid Solvents Convert Sugars to 5-Hydroxymethylfurfural. *Science* **2007**, *316* (5831), 1597-1600.
32. Qi, X.; Watanabe, M.; Aida, T. M.; Smith, R. L., Synergistic conversion of glucose into 5-hydroxymethylfurfural in ionic liquid–water mixtures. *Bioresource Technology* **2012**, *109*, 224-228.
33. Sun, A.; Zhang, J.; Li, C.; Meng, H., Gas Phase Conversion of Carbon Tetrachloride to Alkyl Chlorides Catalyzed by Supported Ionic Liquids. *Chinese Journal of Chemistry* **2009**, *27* (9), 1741-1748.
34. Dharaskar, S. A.; Varma, M. N.; Shende, D. Z.; Yoo, C. K.; Wasewar, K. L., Synthesis, Characterization and Application of 1-Butyl-3 Methylimidazolium Chloride as Green Material for Extractive Desulfurization of Liquid Fuel. *The Scientific World Journal* **2013**, *2013*, 395274.
35. Tao, D.-J.; Wu, J.; Wang, Z.-Z.; Lu, Z.-H.; Yang, Z.; Chen, X.-S., SO₃H-functionalized Brønsted acidic ionic liquids as efficient catalysts for the synthesis of isoamyl salicylate. *RSC Advances* **2014**, *4* (1), 1-7.
36. Bokade, V. V.; Yadav, G. D., Heteropolyacid supported on montmorillonite catalyst for dehydration of dilute bio-ethanol. *Applied Clay Science* **2011**, *53* (2), 263-271.

37. Widjaya, R. R.; Juwono, A. L.; Rinaldi, N., Chromium Pillared Montmorillonite as Catalyst for Liquid Biofuel Conversion. *Asian Journal of Applied Sciences* **2019**, 7 (5).
38. Varadwaj, G. B. B.; Rana, S.; Parida, K. M., Amine functionalized K10 montmorillonite: a solid acid–base catalyst for the Knoevenagel condensation reaction. *Dalton Transactions* **2013**, 42 (14), 5122-5129.
39. Zhang, L.; Xi, G.; Chen, Z.; Jiang, D.; Yu, H.; Wang, X., Highly selective conversion of glucose into furfural over modified zeolites. *Chemical Engineering Journal* **2017**, 307, 868-876.

APPENDIX

Figure S1: ^1H NMR spectra (500.0 MHz 25 °C, DMSO- d_6) of glucose.Figure S2: ^1H NMR spectra (500.0 MHz 25 °C, DMSO- d_6) of levulinic acid.

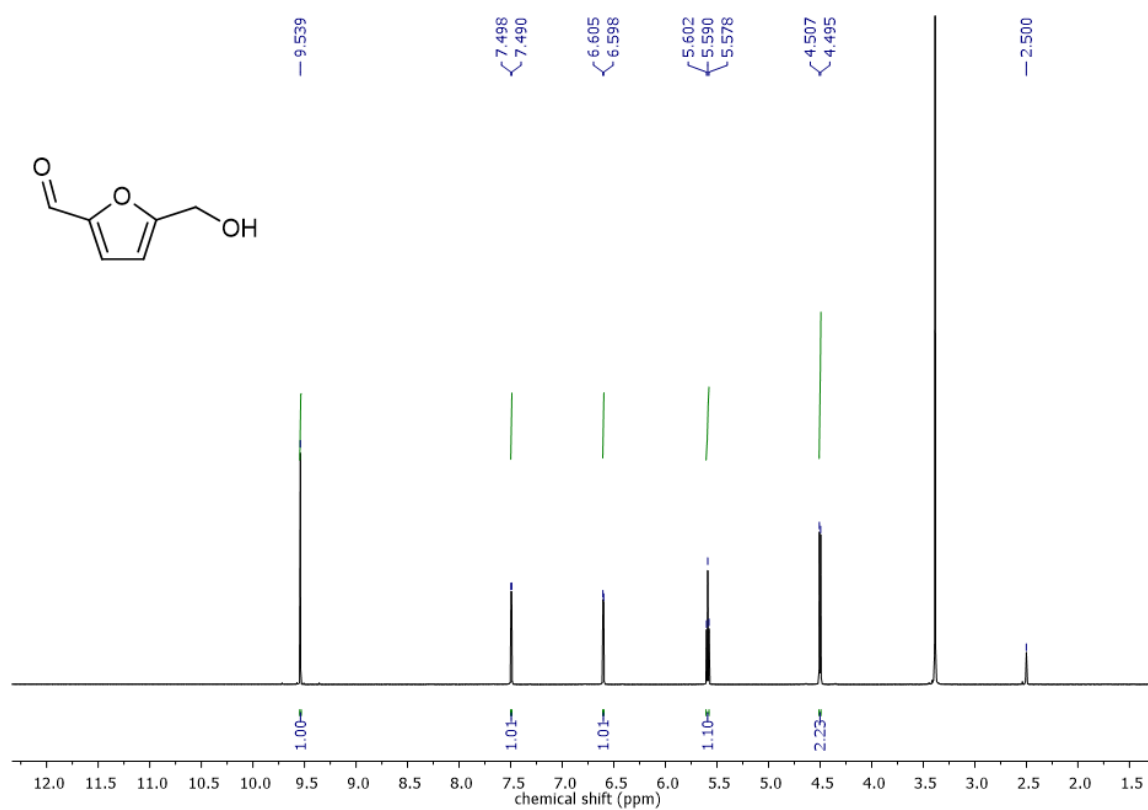


Figure S3: ^1H NMR spectra (500.0 MHz 25 $^\circ\text{C}$, DMSO-d_6) of HMF.

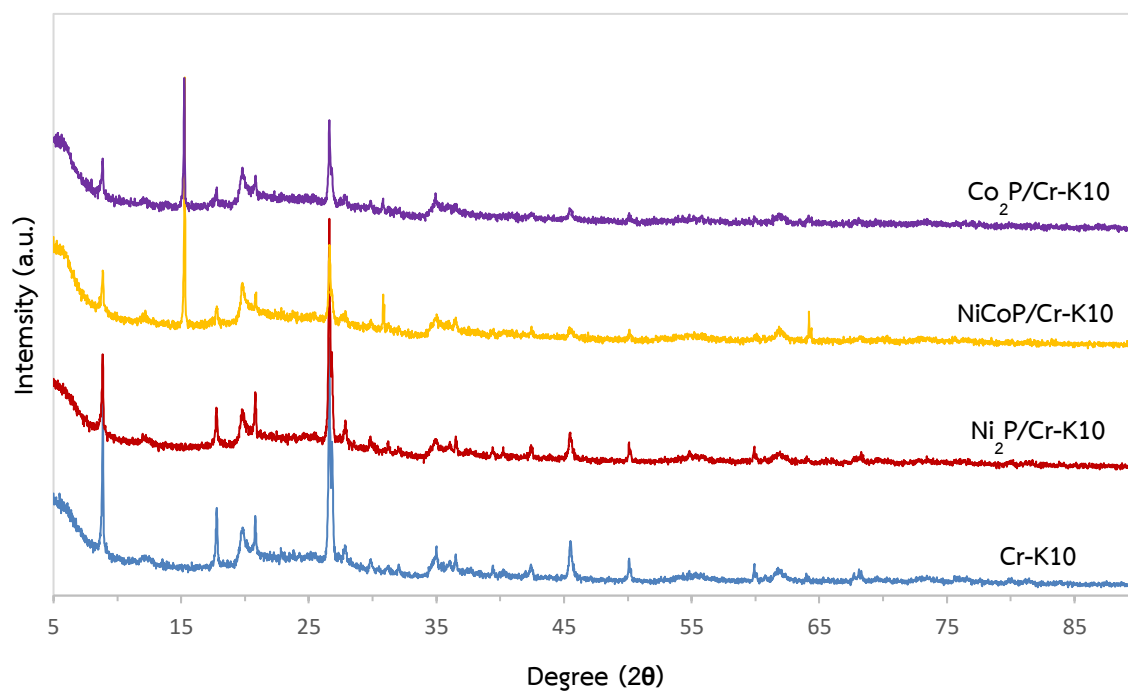


Figure S4: XRD pattern of the synthesized $\text{Ni}_2\text{P/Cr-K10}$, NiCoP/Cr-K10 and $\text{Co}_2\text{P/Cr-K10}$.

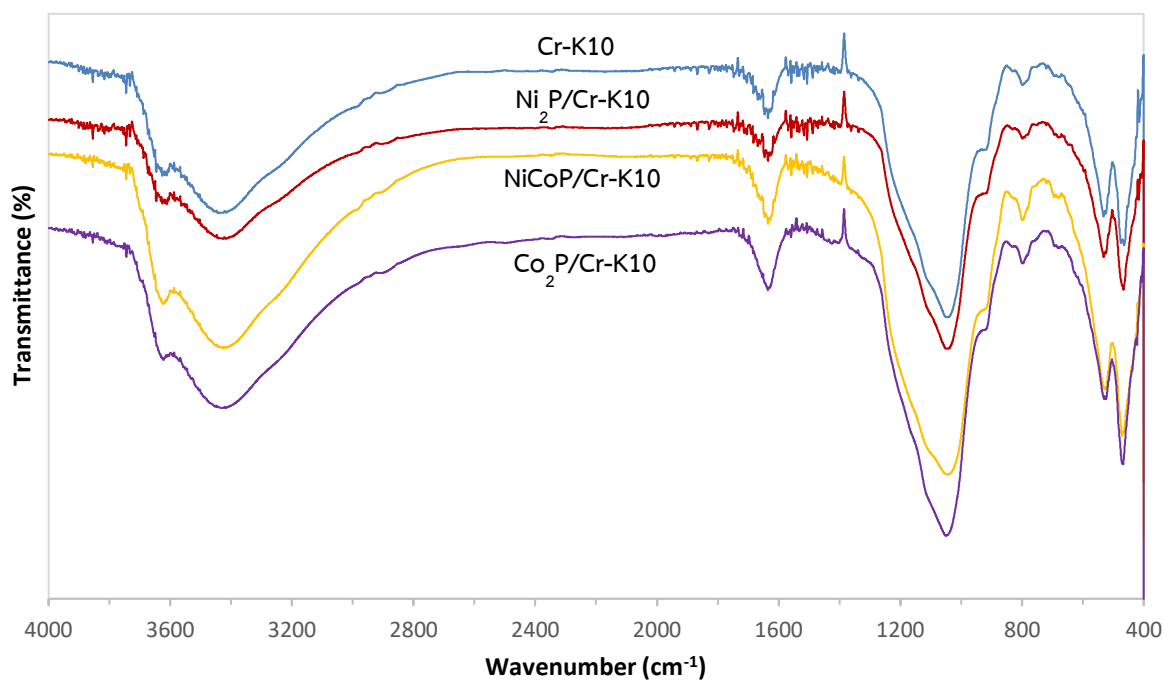


Figure S5: FT-IR spectra of the synthesized Ni₂P/Cr-K10, NiCoP/Cr-K10 and Co₂P/Cr-K10.

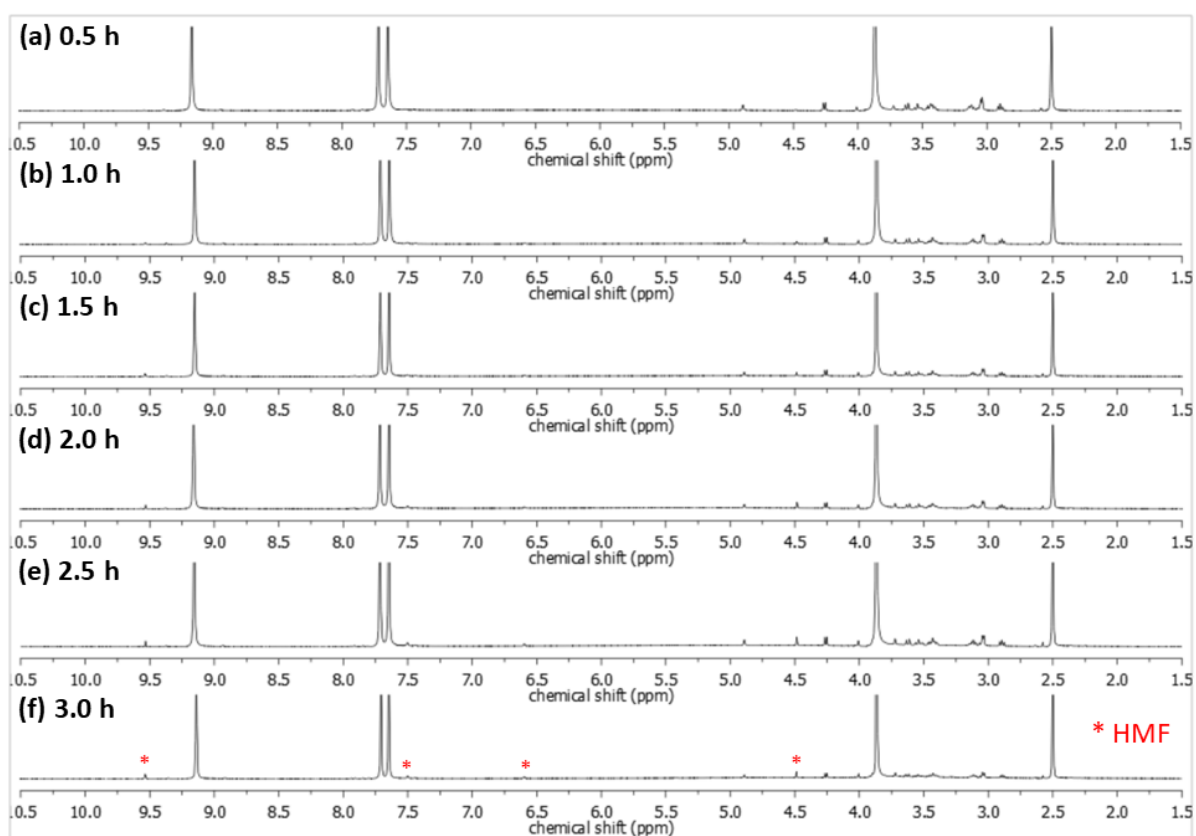


Figure S6: Stacked ¹H NMR spectra (500.0 MHz 25 °C, DMSO-d₆) of glucose conversion for (a) 0.5 (b) 1 (c) 1.5 (d) 2 (e) 2.5 (f) 3 h using Cr-K10 catalyst in [HMIM]Cl as media.

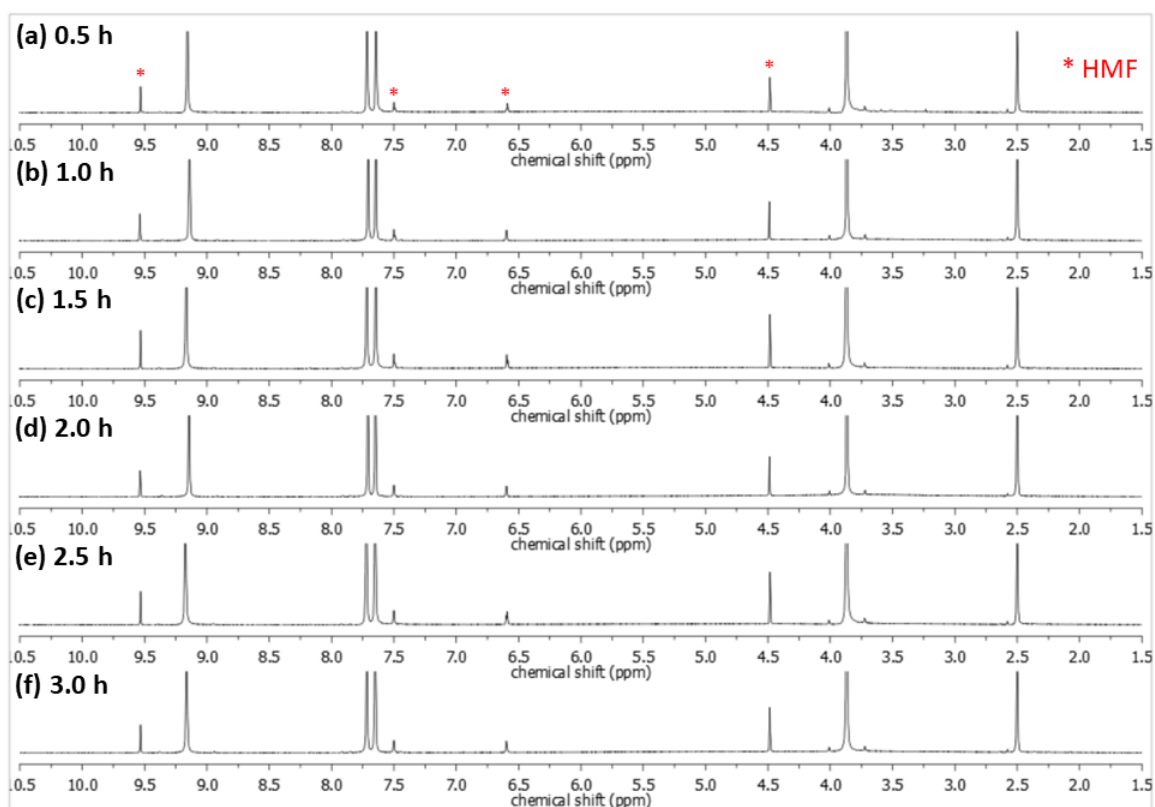


Figure S7: Stacked ^1H NMR spectra (500.0 MHz 25 $^\circ\text{C}$, DMSO-d_6) of fructose conversion for (a) 0.5 (b) 1 (c) 1.5 (d) 2 (e) 2.5 (f) 3 h using Cr-K10 catalyst in [HMIM]Cl as media.

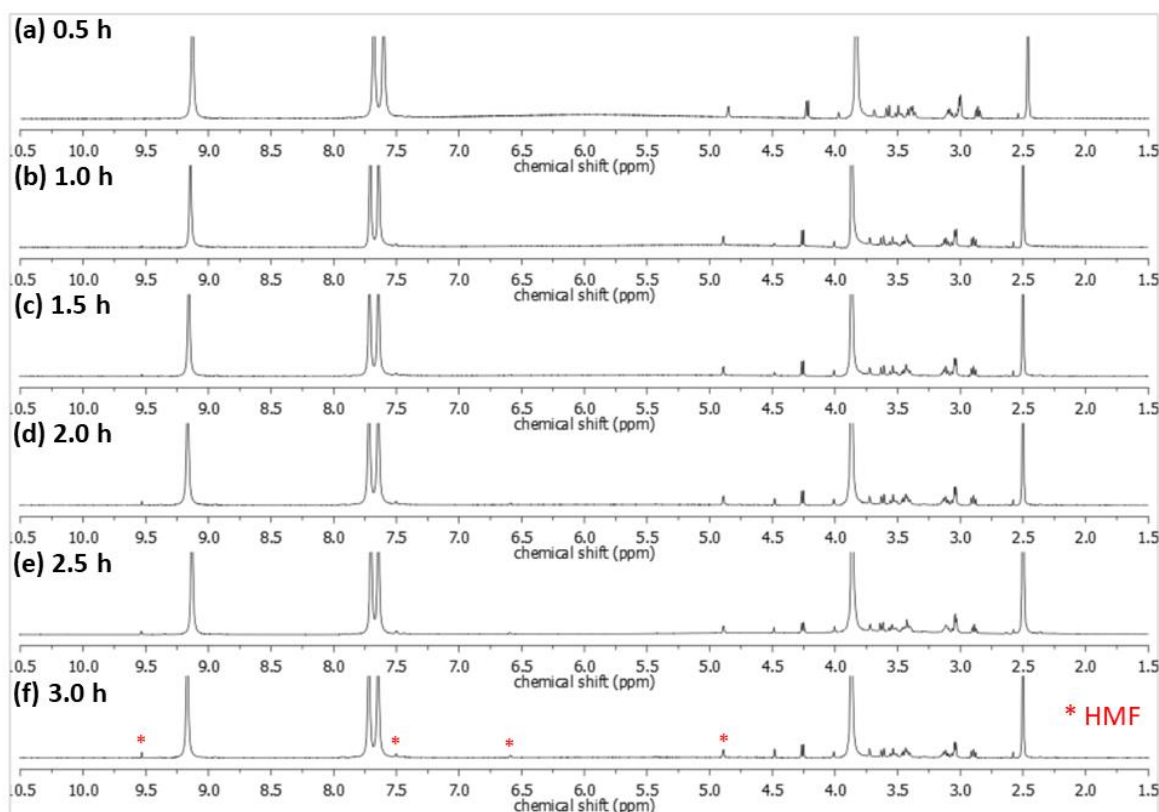


Figure S8: Stacked ^1H NMR spectra (500.0 MHz 25 $^\circ\text{C}$, DMSO-d_6) of glucose conversion for (a) 0.5 (b) 1 (c) 1.5 (d) 2 (e) 2.5 (f) 3 h using $\text{Ni}_2\text{P/Cr-K10}$ catalyst in [HMIM]Cl as media.

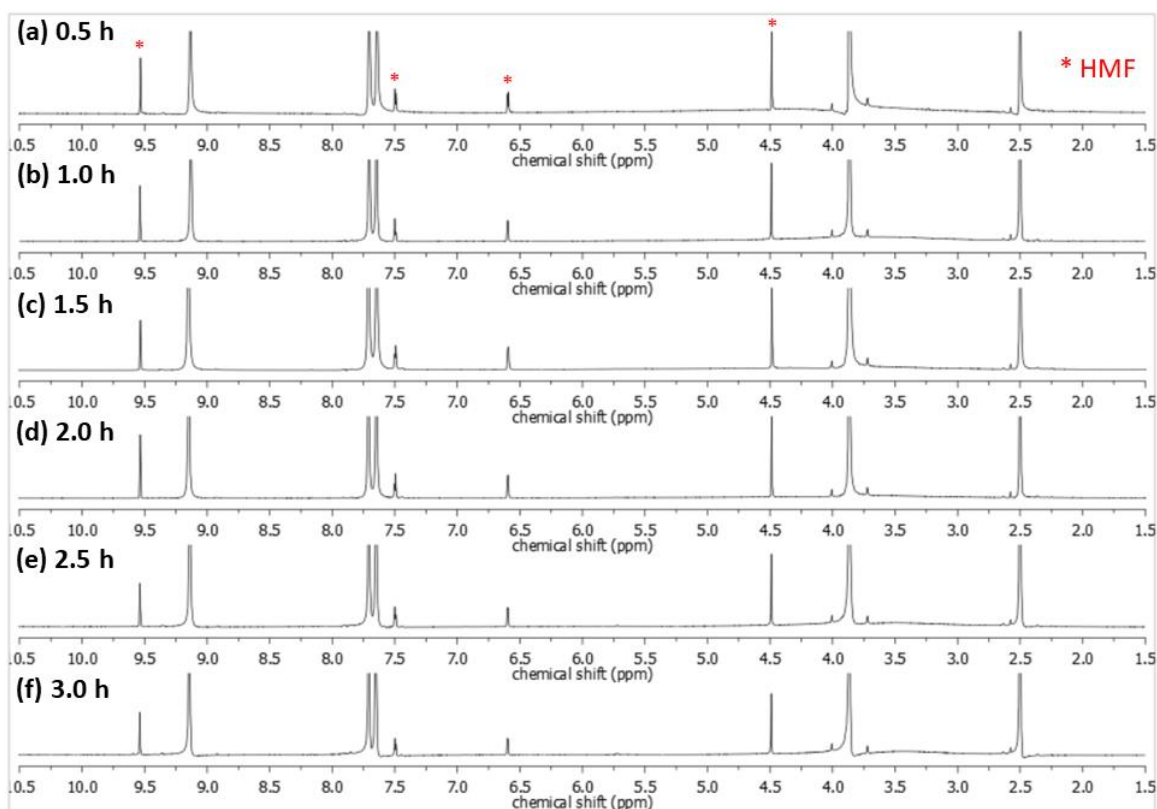


Figure S9: Stacked ^1H NMR spectra (500.0 MHz 25 °C, DMSO-d_6) of fructose conversion for (a) 0.5 (b) 1 (c) 1.5 (d) 2 (e) 2.5 (f) 3 h using $\text{Ni}_2\text{P/Cr-K10}$ catalyst in $[\text{HMIM}]\text{Cl}$ as media.

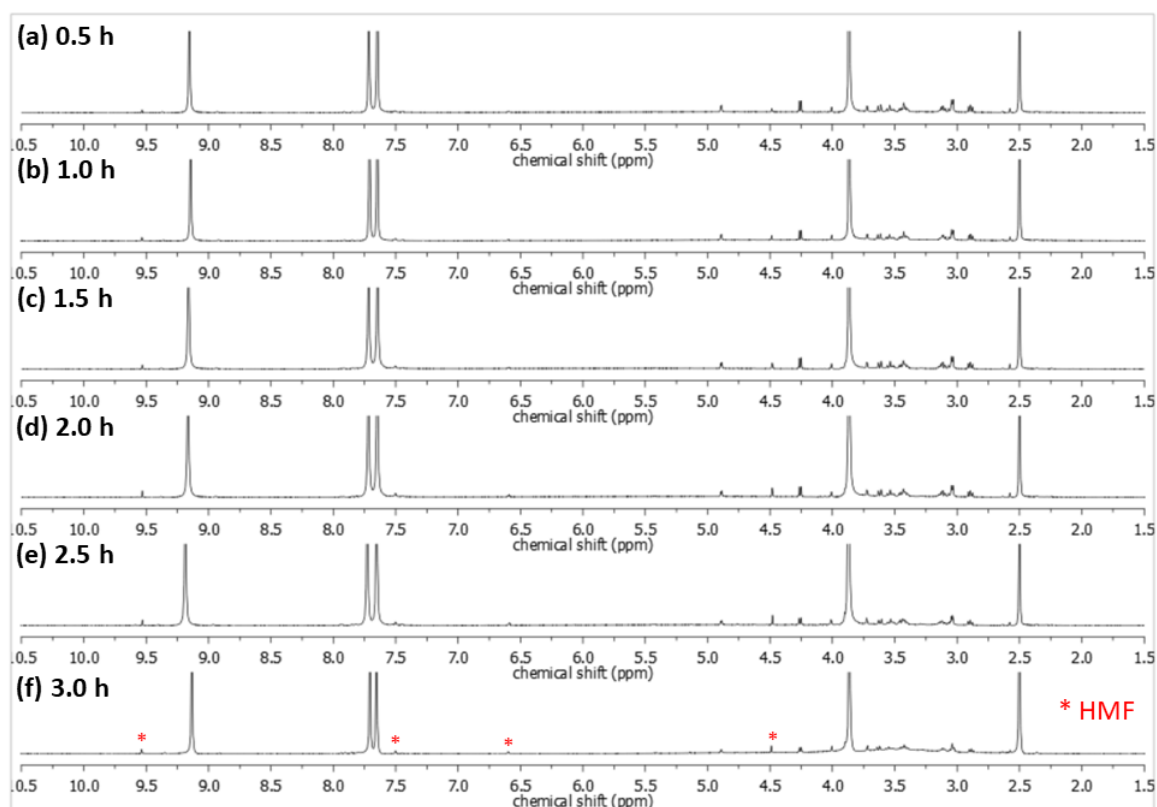


Figure S10: Stacked ^1H NMR spectra (500.0 MHz 25 °C, DMSO-d_6) of glucose conversion for (a) 0.5 (b) 1 (c) 1.5 (d) 2 (e) 2.5 (f) 3 h using Ni_2P mixed with Cr-K10 catalyst in $[\text{HMIM}]\text{Cl}$.

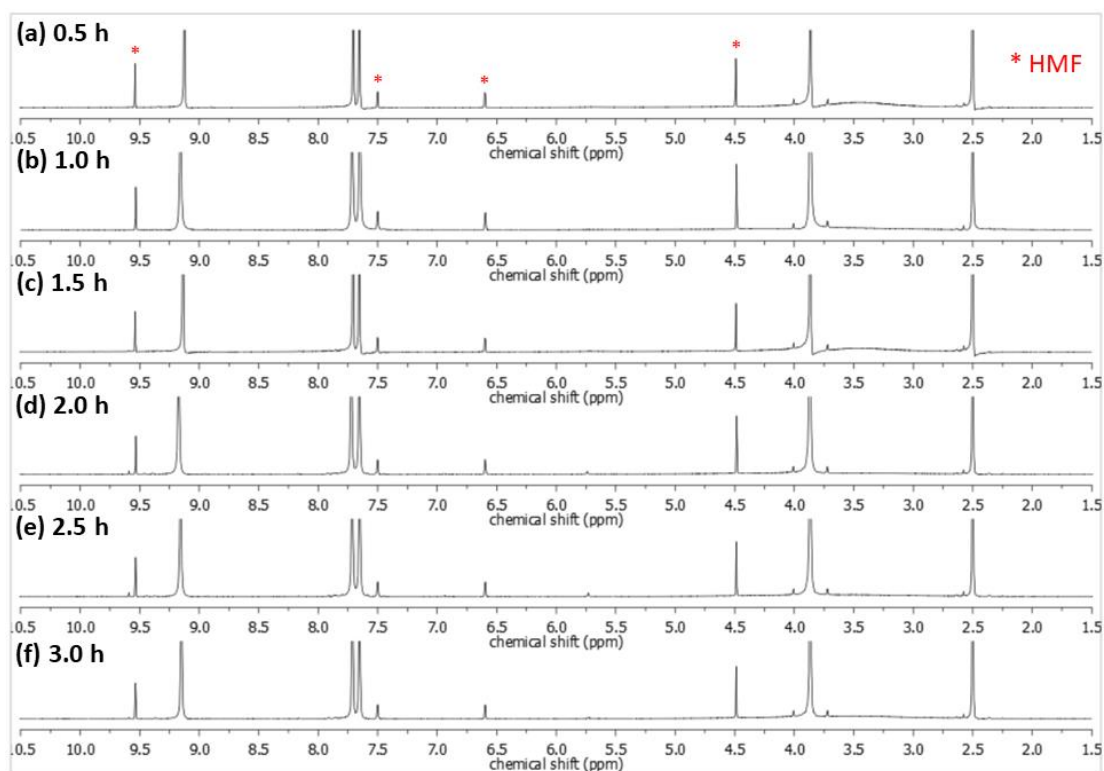


Figure S11: Stacked ^1H NMR spectra (500.0 MHz 25 °C, DMSO-d_6) of fructose conversion for (a) 0.5 (b) 1 (c) 1.5 (d) 2 (e) 2.5 (f) 3 h using Ni_2P mixed with Cr-K10 catalyst in [HMIM]Cl.

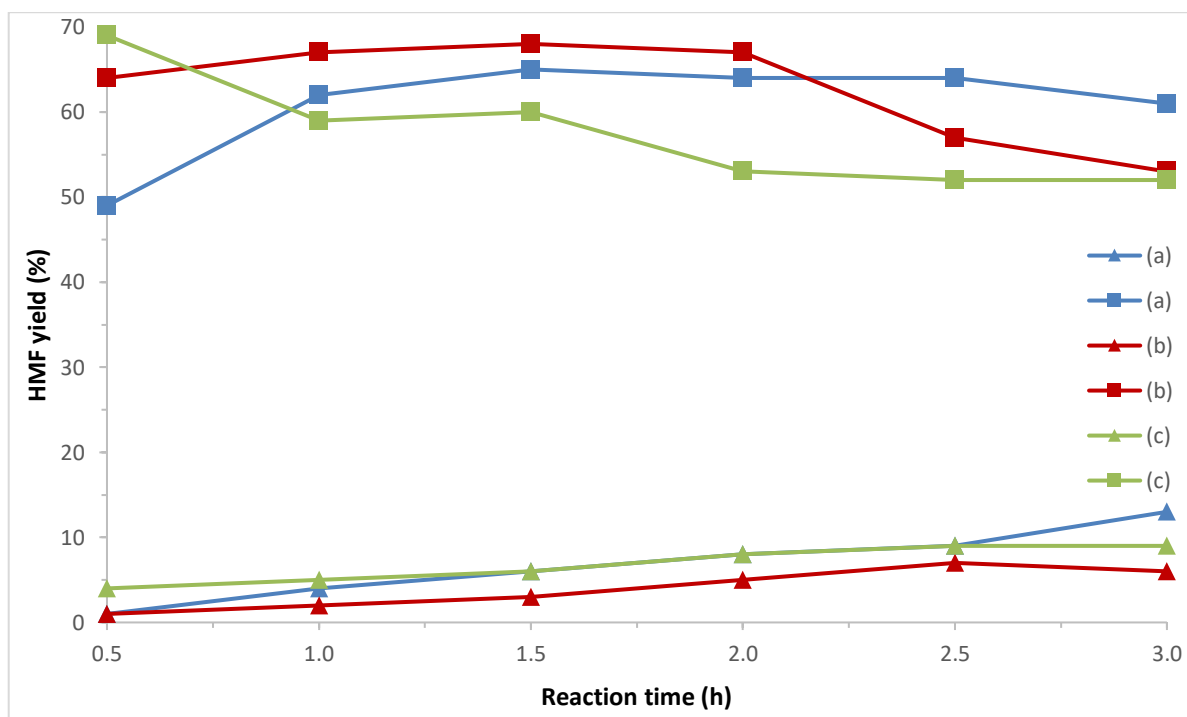


Figure S12: Catalytic conversion of glucose (Δ) and fructose (\square) into HMF in [HMIM]Cl medium using (a) Cr-K10 (b) $\text{Ni}_2\text{P}/\text{Cr-K10}$ (c) Ni_2P mixed with Cr-K10 catalyst. Reaction conditions: Feedstock (50 mg) and catalyst (50 mg) were added in [HMIM]Cl medium, and the reaction was carried out at 120 °C.

VITA

Miss Patitta Preedanorawut was born on August 18th, 1998 in Bangkok, Thailand. She got a high school diploma from Bodindecha (Sing Singhaseni) School in Mathematics-Science program, Bangkok in 2016. She started as a bachelor's degree student in Department of Chemistry, Faculty of Science, Chulalongkorn University in academic year 2017 under Development and Promotion of Science and Technology Talents Project (DPST) scholarship. Her current address is 433 Soi. Tessaban 13, Sukhumvit Road, Paknam, Mueang, Samutprakan, 10270.